공학박사 학위논문

Catalytic Conversion of Macroalgae-derived Alginates to Valuable Organic Compounds under Hydrothermal Conditions

고부가가치 유기화합물 생산을 위한 해조류 유래 알지네이트의 촉매적 수열반응 연구

2015년 8월

서울대학교 대학원

화학생물공학부

전원진

Abstract

Catalytic Conversion of Macroalgae-derived Alginates to Valuable Organic Compounds under Hydrothermal Conditions

Wonjin Jeon

School of Chemical and Biological Engineering

The Graduate School

Seoul National University

Recently, marine biomass is gaining attraction as a promising renewable feedstock for production of biofuels and valuable chemicals. This aquatic biomass including microalgae and macroalgae has important advantages such as easy cultivation on non-arable land, a rapid growth rate and its lignin-free composition, in comparison with corn, sugarcane and lignocellulosic biomass. Microalgae is extensively studied for producing biodiesels based on the high lipid content in maicroalgae. On the other hand, macroalgae contains abundant carbohydrate components such as alginate and mannitol instead of lipid, which can be applied in production of bio-oil, volatile fatty acids (VFAs) and bio-alcohol. Alginate is one of the main components of macroalgae, especially brown seaweeds. It is composed of two monomeric subunits, β-D-mannuronic acid and α-L-guluronic acid, connected by β-1,4-glycosidic bonds. This cellulose-like structure of alginate has great potential for production of valuable chemicals via thermochemical or biological conversion processes. Among various conversion processes, hydrothermal process using hot-compressed water is

promising, since it is a low-cost and eco-friendly biorefinery technique valorizing biomass-derived carbohydrate materials.

The hydrothermal conversion of alginate was performed at reaction temperatures from 150 to 200 °C as a function of pH in order to investigate the effects of acidity and basicity on the production of value-added chemicals. The pH value of aqueous medium was used as a quantitative standard indicating acidity and basicity. A base-catalyzed reaction at pH 13 enahnced the decomposition of alginate, resulting in the production of lactic acid, fumaric acid and malic acid as major species. At pH 1, monomers (mannuronic acid and guluronic acid), furfural and glycolic acid were predominantly produced by the acid-catalyzed hydrothermal decomposition of alginate. Increasing the reaction temperature promoted both the acid- and base-catalyzed reactions, indicating that hot-compressed water can play a role of catalyst itself due to the increasing ion product (K_w). This study demonstrates that optimizing the acidity, basicity and temperature is significantly important for the efficient conversion of alginate to valuable products.

To study the effect of catalysts on the production of lactic acid from alginate, metal oxides were employed as solid base catalysts. The CaO catalyst exhibited the highest catalytic performance, yielding 14.66 % lactic acid at 200 °C for 6 h, while other metal oxide catalysts showed little activity. The yield of lactic acid was proportional to the number of Brønsted bases (OH^-) in an aqueous medium, measured by titration of metal oxides. The catalytic activity of CaO catalyst was maintained for two subsequent reaction cycles and the deactivated catalyst was successfully regenerated by calcination. The deactivation of the CaO catalyst during subsequent repeated uses arose from decrease in the number of available active sites

providing both Lewis acid site and Brønsted basic site, by covering the active sites with various byproducts. Plausible reaction pathway for the catalytic conversion of alginate to lactic acid over CaO was also discussed. The effect of metal oxide catalysts on the depolymerization of alginate was also analyzed based on the molecular weight distribution of products.

The catalytic effect of metal cations on the hydrothermal production of furfural from alginic acid was investigated with using various metal ions as catalysts. Among the metal ions, Cu (II) ions demonstrated the highest furfural yield (13.19 %) at 200 °C for 30 min. As the reaction temperature increased from 160 to 220 °C, the production of furfural was enhanced, however, the maximum furfural yield at each reaction temperature decreased after certain reaction times due to the conversion of furfural to humins or organic acids. The yield of furfural was strongly dependent upon metal ion concentration and the optimal concentration of Cu (II) ions was 0.01 M. In addition to furfural, lactic acid, glycolic acid and formic acid were produced in different amounts. The effect of Cu (II) ion on the depolymerization of alginate was studied with gel permeation chromatography (GPC) analysis. A plausible reaction pathway of furfural production catalyzed by Cu (II) ions was proposed.

Keywords: alginate, hydrothermal reaction, homogeneous catalysis, heterogeneous catalysis, organic acids, furfural

Student Number: 2012-30259

Contents

List of Tables

List of Figures

Chapter 1. Introduction

The utilization of fossil fuels, such as coal, petroleum and natural gas, has provided the large amounts of energy and useful chemicals for industry and our daily lives, however, it has caused serious impacts on the environment. For example, carbon dioxide discharging from burning the fossil fuels exacerbates the greenhouse effect, and acidic compounds produced by the use of fossil fuels damage our natural areas and built environment in a form of acid rain [1-3]. In addition, the depletion of fossil fuels has been accelerated due to the high dependency in energy consumption for several decades [4, 5]. The environmentally adverse effects and non-renewability of the fossil fuels lead to vigorous investment in exploring alternative renewable resources like biomass.

1.1 Marine biomass

The first-generation biomass, such as corn and sugarcane, has been widely utilized in development of biofuel production, such as bioethanol. The conversion process of crops to biofuels is simple and inexpensive, however, the large consumption of edible crops for the biofuel production leads to critical problems like inflation of food prices and pollution of agricultural land by using fertilizers [6]. Although the second-generation biomass, lignocellulosic biomass including wood waste and grasses, is non-edible and cheap as a biomass feedstock, the biofuel production using the lignocellulosic biomass has considerable limitations such as high capital cost and its recalcitrant structures resistant to biological and chemical treatments [7, 8].

As the third-generation biomass, marine biomass including macroalgae and

microalgae is gaining great attention as a renewable resource for development of biofuels and valuable platform chemicals. Comparing to the first- and second-generation biomass, the aquatic biomass has many advantages like lignin-free structure, non-edibility and the high growth rate in the absence of fertilizers. As listed in Table 1-1, Giant brown kelp, a representative macroalgae, does not contain lignin, while woody biomass is composed of more than 25% of lignin. The lignin component has very recalcitrant structure and it is difficult to degrade the lignin-based materials via biological or chemical treatments [9, 10]. The marine biomass is mainly comprised of protein, liqid and carbohydrates, favorable for the production of high value-added products such as biodiesel, bio-oil, and various organic chemicals [11-13]. Microalgae contains abundant lipids rather than carbohydrates and this composition is advantageous for biodiesel production via biochemical conversions of microalgae [14-16]. On the other hand, macroalgae is mainly composed of carbohydrates, such as alginate, laminarin and mannitol, which can be applied to production of bio-oil and useful platform chemicals like furan compounds and organic acids.

Table 1-1 Organic components and ash in representative bioimass [17].

Biomass type	**Marine**	**Herbaceous**	**Woody**	**Waste**
Name	Giant brown kelp	Bermuda grass	Pine	Refuse-derived fuel
Celluloses	4.8	31.7	40.4	65.6
Hemicellulose	-	40.2	24.9	11.2
Lignin	-	4.1	34.5	3.1
Mannitol	18.7	-	-	-
Alginate	14.2	-	-	-
Laminarin	0.7	-	-	-
Fucoidin	0.2	-	-	-
Crude protein	15.9	12.3	0.7	3.5
Ash	45.8	5.0	0.5	16.7

1.2 Alginate

Alginate is one of the major components in marine biomass, especially brown seaweeds. It can be obtained by the acidic extraction of the brown seaweeds [18]. In general, alginate is widely utilized in food, pharmaceutical and cosmetics as an additive for gelling, viscosifying and stabilizing various products. For example, sodium alginate is added into the production of ice creams in order to control the creamy textile and suppress the crystallization of creams in a manufacturing process. The scientific approach has been achieved from the early 20th century. The biopolymer is composed of two monomeric units, β-D-mannuronic acid and α-L-guluronic acid via the 1,4-glycosidic linkage [19]. Before 1940, it was known that alginate contained mannuronic acid only by the glycosidic bond. However, Fischer and Dörfel firstly found that guluronic acid is also included in alginate structure with mannuronic acid [20]. The ratio between two kinds of monomers is depending on the species of marcroalgae, cultivation environment and season. The structure of alginate is very similar with that of cellulose, a main component of lignocellulosic biomass, except an extra carboxylic group at monomeric units of alginate, as shown in Figure 1-1. Based on the structural similarity, both alginate and cellulose are hydrolyzed to its monomers via the cleavage of the glycosidic linkage [21-24]. This cellulose-like structure of alginate has great potential for the production of valuable chemicals from biological or chemical conversion processes.

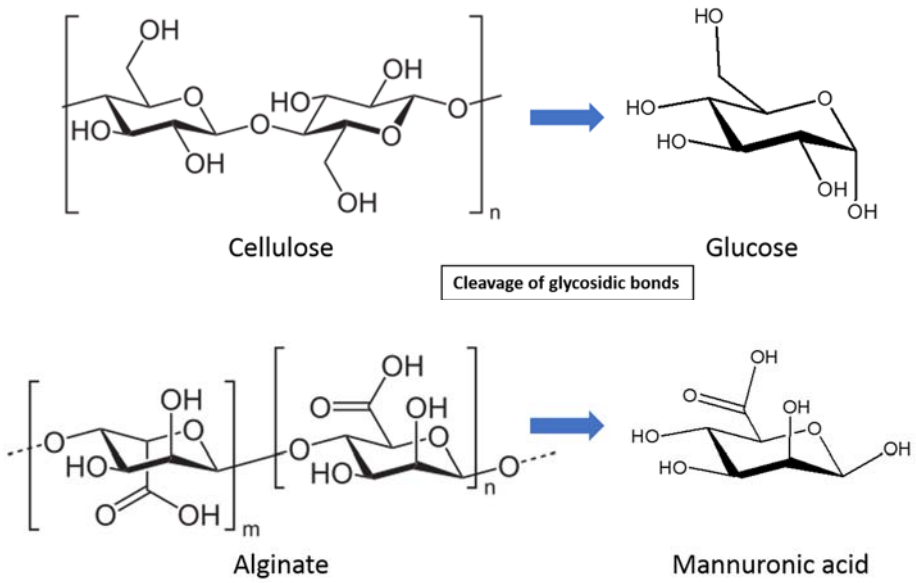

Figure 1-1. Polymeric and monomeric structure of alginate and cellulose.

1.3 Hydrothermal techniques

Hydrothermal processing is generally divided to liquefaction, catalytic gasification and high-temperature gasification, based on the processing temperature and pressure as shown in Figure 1-2 [25]. The hydrothermal liquefaction occurs at reaction temperatures from 200 °C to 350 °C under various pressure conditions and the aqueous reaction medium in the temperature range is called as hot-compressed water [26]. The reaction conditions for the hydrothermal liquefaction can transform biomass-derived carbohydrates [27]. For example, cellulose, glucose and other monosaccharides can be converted to furans, organic acids and various carbonyl compounds, depending on catalysts [28-34]. Over 350 °C, the hot-compressed water is in the supercritical region and thus gasification of biomass is predominant, yielding gaseous products, such as hydrogen, carbon dioxide and methane [35-37].

The reaction pathways in the hydrothermal conditions at different temperatures are strongly depending on physical and chemical properties of the hot-compressed water. Those properties are varied by changing temperature and pressure of water as listed in Table 1-2. In closed reaction systems, the reaction temperature is a key factor determining the reaction pressure, which can change the physicochemical properties of water such as ion product ($K_W=[H^+][OH^-]$) and dielectric constant [26]. For example, the dissociation of water molecules to protons (H^+) and hydroxyl ions (OH^-) is promoted in the aqueous medium as the reaction temperature increases, leading to increase of ion product. These two ions can catalyze hydrolysis, dehydration and isomerization of carbohydrate molecules in spite of the absence of additional

catalysts. Protons and hydroxyl ions acting as Brønsted acid and base promote acid- and base-catalyzed reactions, repectively. For instance, cellulose is mainly converted to hydroxymethylfufural (HMF) and lactic acid under the acid and base catalysts, respectively [23, 38]. In addition to the ion product, dielectric constant is also important in the hydrothermal reaction of biomass-derived carbohydrates. The deceasing dielectric constant by increasing the reaction temperature enhance the hydrophilic interactions between water and carbohydrate materials, enhancing the hydrothermal reactions such as hydrolysis, dehydration and retro-aldol condensation [39]. In addition, the aqueous reaction medium is suitable for eco-friendly and inexpensive hydrothermal process.

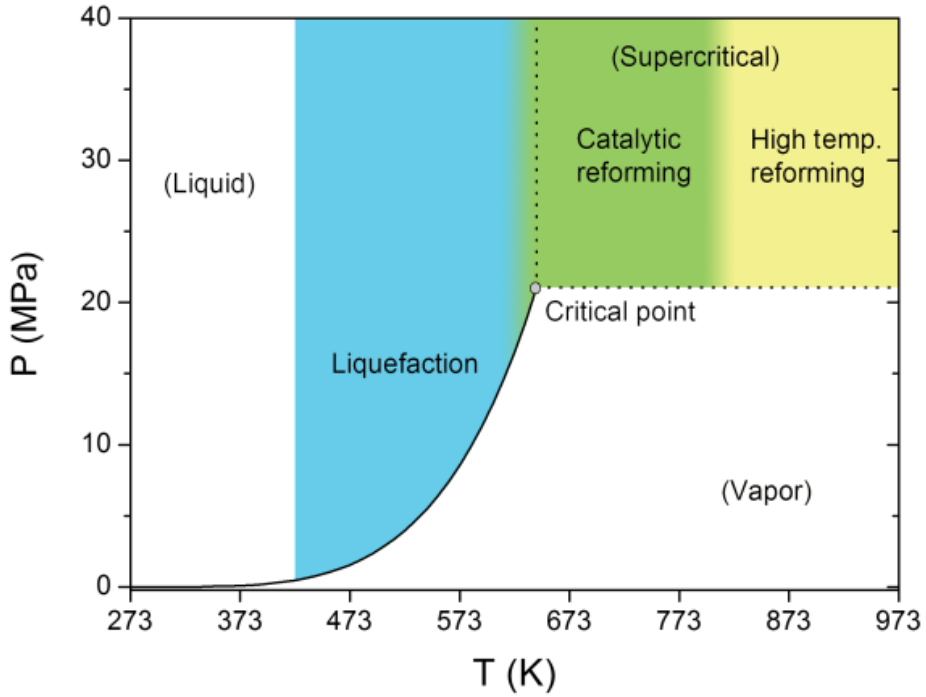

Figure 1-2. Hydrothermal processing regions based on the phase diagram of water [25].

Table 1-2. Physical and chemical properties of water in different temperature and pressure windows [26].

	Ambient temperature	**Subcritical water**	**Supercritical water**
Temperature [°C]	0–100	100–374	> 374
Vapor pressure [MPa]	0.003 (24 °C)	0.1 (100 °C)–22.1 (374 °C)	> 22.1
Aggregate state	Liquid	Liquid	No phase separation
Density [g cm^{-3}]	0.997 (25 °C)	0.692 (330 °C, 30 MPa) 0.958 (101 °C, 0.11 MPa)	Between gas and liquid densities
Viscosity [mPa s]	L: 884 G: 9.9 (25 °C)	L: 277 G: 12.3 (101 °C) L: 50.4 G: 30.7 (371 °C)	Low
Heat capacity CP [J g^{-1} K^{-1}]	L: 4.2 G: 2.0 (25 °C)	L: 4.2 G: 2.1 (101 °C) L: 69 G: 145 (371 °C)	1300 (400 °C, 25 MPa)
Dielectric constant	78.5 (25 °C, 0.1 MPa)	27.1 (250 °C, 5 MPa) 18.2 (330 °C, 30 MPa)	5.9 (400 °C, 25 MPa) 10.5 (400 °C, 50 MPa)
Compressibility	No	Slightly increased, but still a liquid (at 370 °C)	Yes
Ion product Kw [mol^2 L^{-2}]	10^{-14} (increasing to 10^{-12} at 100 °C)	Increases from 10^{-12} (100 °C) to 10^{-11} (300 °C)	Below 10^{-20} (400 °C) Below 10^{-23} (550 °C)

L: liquid phase, G: gas phase

1.4 Objectives

Although the hydrothermal treatment of alginate has been studied from the early 20th century, the effect of catalyst on the hydrothermal decomposition of alginate was not systematically investigated. This thesis mainly consists of studying the effect of catalyst on the hydrothermal conversion of alginate in order to propose promising catalysts for the selective production of high value-added chemicals. The relationship between the acidity (or basicity) of reaction medium and the product distribution is investigated in Chapter 2. The relationship is helpful for understanding the effect of acidity and basicity on the hydrothermal decomposition of alginate. Based on the results in Chapter 2, various catalysts are introduced with the purpose of selectively producing furfural or lactic acid. In Chapter 3, metal oxides are employed as solid base catalysts in order to enhance the production of lactic acid from alginate. The correlation between the physical and chemical properties of metal oxides and the yield of lactic acid is presented to suggest the active sites of catalysts in the production of lactic acid. In addition, the method for reuse and regeneration of used catalysts is proposed. In Chapter 4, various metal cations are evaluated as a catalyst for the selective conversion of alginic acid to furfural in the hydrothermal conditions. A plausible reaction pathway for the production of furfural from alginate is proposed in order to explain the catalytic role of metal cations in the reaction.

Chapter 2. The Effects of pH on the Hydrothermal Decomposition of Alginate

2.1 Introduction

Hydrothermal treatment is a useful method to convert biomass-derived carbohydrates to valuable chemicals with using hot-compressed water as a reaction medium. The hydrothermal conversion of carbohydrates, such as lignocellulosic compounds, can be completed within a few hours via relatively simple procedures [23, 38, 40-42]. In addition, water is a cheap, sustainable and eco-friendly reaction medium compared to expensive and toxic organic solvents [26].

Alginate, composed of β-D-mannuronic acid and α-L-guluronic acid, has a cellulose-like structure, which has great potential for the hydrothermal conversion of alginate. As depicted in Figure 2-1, the monomers of alginate are connected by β-1,4-glycosidic bonds and the linkages are selectively broken by hydrolysis in hydrothermal reaction conditions, analogous to hydrolysis of cellulose to glucose [43-48]. After the hydrolysis step, the monomers can be converted to organic compounds, mainly organic acids, via breaking of the C-C or C-O bonds within the monomeric subunits [49-51]. Hydrothermal conversion of cellulose into valuable organic compounds has been extensively investigated [52-57], however, hydrothermal treatment of alginate has hardly performed during the past decades. Recently, Aida et al. reported the production of monomers and organic acids under subcritical and supercritical water conditions [50, 51]. They studied the effect of reaction temperature (150–400 °C) on the conversion of alginate into its monomers and monomer-derived

organic acids, such as monocarboxylic and dicarboxylic acids. The effect of homogeneous catalysts (such as mineral acids and alkali solutions) on hydrothermal degradation of alginate was investigated between the 1960s and 1980s [22, 49, 58, 59], but the reaction conditions were limited and quantification of the furfural and organic acids was insufficient. Moreover, the effect of acid and base catalysts on the conversion of alginate at temperatures higher than 150 °C remains unknown.

In this study, the initial acidity or basicity of the aqueous reaction medium were controlled by adding Arrhenius acid or base to water, in order to better understand the influence of acid- and base-catalyzed reactions on the hydrothermal decomposition of alginate. The pH value of reaction solvent was used as a standard indicating the acidity and basicity. The reaction was performed in a range of temperature from 150 to 250 °C to understand the role of catalyst at the different reaction temperatures. Formic acid, acetic acid, glycolic acid, lactic acid, fumaric acid, succinic acid, malic acid and furfural are selected as target products, because these C_1–C_5 organic compounds can be utilized as platform chemicals for producing high value-added chemicals.

2.2 Experimental

2.2.1 Preparation of reaction solvents

To control the pH level of aqueous medium, hydrogen chloride (Junsei Chemical) and sodium hydroxide (Sigma-Aldrich) were used as Arrhenius acid and base, respectively. For preparation of the acidic solvents, hydrogen chloride was added to distilled water until the pH of the solvents reached 1 and 3. Likewise, sodium hydroxide and distilled water were used to produce basic solvents of pH 11 and 13. All organic acids were purchased from Sigma-Aldrich, except fumaric acid which was obtained from Tokyo Chemical Industry. Standard chemicals of alginate monomers, mannuronic acid and guluronic acid, were purchased from Qingdao BZ Oligo Biotech, China (purity > 98%). Sodium alginate obtained from Sigma-Aldrich was used as a reactant in the hydrothermal depolymerization reaction with no mechanical pretreatment like ball-milling. Cellulose was purchased from Sigma-Aldirich and mechanically treated with a ball-milling machine for 20 h to reduce the particle size (≤ 250 μm) in order to enhance the reactivity, since cellulose is insoluble to water in comparison with sodium alginate.

2.2.2 Hydrothermal treatment of alginate

A tubular batch reactor (SUS316) was used to conduct the hydrothermal conversion of sodium alginate. A molten salt including the mixture of alkali metal nitrates was utilized for heating the reactor. First, sodium alginate (60 mg) and aqueous solvent (3 mL) were loaded together into the reactor, which had

an inner volume of 6 mL. Second, the inside space of reactor was purged with N_2 gas (99.999%). Next, the reactor was immersed in the molten salt bath and taken into a cold-water bath immediately after the desired reaction time. The reactor reached the target temperatures (150, 200 and 250 °C) within 150 s. It was presumed that the aqueous solvent exists as saturated water in these reaction conditions, based on water properties calculated with the equation of state. The reaction time was recorded from the initial time that a temperature sensor in the reactor first detected the desired reaction temperature. Finally, the final products were neutralized, centrifuged and diluted prior to product analysis.

2.2.3 Product analysis

Final products were identified with a GC-MS System (Clarus 680/600T, Perkin-Elmer) equipped with an Agilent DB-5MS column. The product samples were lyophilized and silylated with a mixture of BSFTA with TMCS (99:1) and pyridine at 65 °C for 2 hr. A result of GC-MS analysis for major products obtained by a reaction at 200 °C and pH 7 for 60 min was presented in Figure 2-2.

Organic compounds were quantified with an Agilent 1200 Series HPLC equipped with two Shodex RSpak KC-811 columns in series. Column oven temperature, flow rate of mobile phase and concentration of phosphoric acid aqueous solution were 40 °C, 1 cm^3/min and 5 mM, respectively. Both refractive index detector (RID, Agilent G1362A) and variable wavelength detector (VWD, Agilent G1314B) were used to cross-check the HPLC analysis for more precise characterization. The wavelength of VWD was set to 210 nm

for analysing organic acids and furan compounds. As a result, each organic compound in the final products was effectively separated as shown in Figure 2-3. Based on data obtained from HPLC analysis, molar yields of products were calculated as:

$$\text{Yield}_i\ (\text{mol}\%) = 100 \times \frac{nC_i}{6} \times \frac{n_i}{n_{ru}}$$

where nC_i = the number of carbon atoms in the organic acid i, n_i = the number of moles of the organic acid i as determined by HPLC analysis, n_{ru} = the initial number of moles of repeating units ($C_6H_7O_6Na$) in the sodium alginate, equal to the mass of sodium alginate divided by 198.

The molecular weight distribution of raw alginate and hydrothermally treated alginate was analyzed by a gel permeation chromatography (GPC) technique. The GPC system (Ultimate 3000, Dionex) was configured with three types of Waters Ultrahydrogel columns: 120, 500 and 1000, in series. Sodium azide solution (0.1M) was used as a mobile phase flowing at 1 mL/min at 40 °C. The GPC calibration was performed using Pullulan with a molecular weight distribution from 342 to 80,500.

^{1}H NMR analysis for raw alginate and final aqueous products was conducted with a 400 MHz spectrometer (JeolJNM-LA400/LFG, JEOL). The ^{1}H NMR spectra were obtained at 80 °C and 128 scans. Liquid parts of final products were lyophilized and then dissolved in D_2O (0.6 mL) containing 3-(trimethylsilyl)propionic-2,2,3,3-d_4 acid sodium salt (0.05 wt%) as an internal standard. At a minimum, tests were executed to ensure reproducibility three times, to obtain reliable results in quantification.

2.3 Results and discussion

2.3.1 Depolymerization of alginate

GPC chromatograms of raw alginates and hydrothermally-treated alginates under various reaction conditions were presented in Figure 2-4. The GPC data were normalized to the intensities of the highest peaks on each chromatogram to compare differences among the chromatograms. Based on the GPC chromatograms, hydrothermal depolymerization of sodium alginate was very sensitive to the reaction temperature and pH of the solvent. For instance, there were no noticeable peaks for the reaction at pH 7 at 250 °C (Figure 2-4-(e)). However, broad and large peaks were observed for the reaction at pH 7 at 150 °C and those peaks gradually shifted toward longer retention times as the reaction time increased (Figure 1-6-b), indicating that the hydrothermal depolymerization of alginate was surely promoted by the increasing temperature. As the reaction temperature increased from 150 to 250 °C, the amount of hydrogen and hydroxyl ions produced by the dissociation of water molecules grew severalfold, accelerating the alginate decomposition via acid- and base-catalyzed hydrolysis by hydrogen and hydroxyl ions, respectively. The effects of catalysts on the alginate degradation were observed as shown in Figure 2-4-(a), (b), (c). At 150 °C, the broad and large peaks for the reaction at pH 7 almost disappeared at pH 1 and 13, indicating that the addition of acid and base catalysts increased the concentrations of hydrogen or hydroxyl ions, and consequently promoted the hydrolysis of alginate. When sodium alginate was degraded with a strong base catalyst at 150 °C, any noticeable peaks were not observed within 25 min of retention time (Figure 2-6-(c)). This suggests that

the strong base catalyst shows better catalytic performance than that of a strong acid catalyst for the hydrothermal degradation of alginate. The raw alginate was largely decomposed after catalyst-free hydrothermal treatment at 250 °C, but small broad peaks were observed within 25 min of the retention time, as shown in Figure 2-4-(e), underlining the effect of catalysts on the depolymerization of alginate.

The weight average molecular weights (M_w) and number average molecular weight (M_n) of products decreased with increasing reaction temperatures from 150 to 250 °C, as listed in Table 2-1. Polydispersity index (PDI) values of products also decreased and converged toward 1 at higher temperatures, strongly suggesting that the depolymerization of alginate into small molecules having similar molecular weights was accelerated at higher temperatures due to vigorous hydrolysis triggered by higher concentrations of hydrogens and hydroxyl ions. The increasing thermal energy gives rise to a decrease of relative dielectric permittivity and an increase in ion products in subcritical water systems [26, 60], which catalyzes the hydrolysis of alginate more effectively. In addition to the reaction temperature, the average molecular weights were drastically reduced when the alginate was depolymerised at 150 °C under acid or base catalysts, as evidenced by GPC chromatograms. The rise of hydrogen and hydroxyl ion concentrations after the addition of catalysts increased the ion products in the hot-compressed water, promoting hydrolysis, nucleophilic substitution and elimination reactions. In particular, the products that decomposed in the presence of a base catalyst exhibited much lower average molecular weights (M_w, M_n) and polydispersity index values than those with an acid catalyst, suggesting that the base-catalyzed elimination (known as a peeling reaction) is more efficient for alginate decomposition. For example,

when the hydrothermal reaction occurred under the base catalyst, the values of M_w and M_n immediately converged to approximately 700 and 520, respectively. This means that the base-catalyzed reaction accelerated multiple and simultaneous cleavages of overall glycosidic bonds in alginate polymer. However, under the acid catalyst at 150 °C, M_w and M_n gradually decreased and PDI values were higher than those values for base-catalyzed reactions, indicating that the rate of alginate depolymerization was relatively low and the acid-catalyzed reaction induced the production of organic compounds with a wide range of molecular weight, compared to the base-catalyzed hydrothermal reaction of alginate at 150 °C.

On the GPC chromatograms, peaks after 27.5 min of retention time indicates the breakdown of mannuronic and guluronic acid into smaller molecules by the cleavage of C-C or C-O linkages in the monomers. When sodium alginate decomposed at pH 1 at 150 °C, the GPC peak from the monomer appeared and then perished as reaction time increased (Figure 2-4-(a)). Coexistence of GPC peaks from the monomer and other smaller products implies that the acid-catalyzed hydrolysis of sodium alginates into monomers and the decomposition of monomers into small organic compounds occur simultaneously. As shown in Figure 2-4-(c), the monomers' peak was not detected within 60 min at pH 13, showing that the decomposition of monomers produced from sodium alginate occurs extremely rapidly in the presence of a strong base catalyst. However, in the catalyst-free reaction (pH 7), the monomers' peak was observed after 60 min of reaction time. These results were consistent with the ^{1}H NMR analysis, as shown in Figure 2-5-(a). The unique peaks for alginate between 4.40 and 5.17 ppm were not observed for the reaction at pH 13 at 150 °C, whereas those peaks clearly appeared when alginate was depolymerised at pH 1 and 7 at

150 °C. Instead of those unique peaks, alternative peaks emerged between 1 to 4 ppm only for the sample treated at pH 13 for 0 min. Both NMR and GPC data demonstrate that sodium alginate is rapidly converted to a complex organic mixture containing hydroxyl and carboxyl groups smaller than monomers at 150 °C under the strong base catalyst.

At 250 °C, the raw alginate was immediately degraded as soon as the reaction initiated under all pH conditions, resulting in that shapes of GPC chromatograms (Figure 2-4-(d), (e), (f)) quickly converged with the average molecular weight values (Table 2-1). The properties of water at 250 °C changed significantly as mentioned above and, as a result, strongly promoted the alginate decomposition regardless of the addition of catalysts. The fast degradation of alginate at the higher temperature was also observed in ^{1}H NMR spectra as shown in Figure 2-5-(b). The characteristic peaks of alginate disappeared completely and, at the same time, numerous other peaks emerged, verifying the production of various organic compounds from alginate decomposition. However, the catalysts were still influential for the molecular distribution of depolymerised alginate. Corresponding with the converged shapes of the chromatograms (Figure 2-4-(d), (e), (f)), the average molecular weights of products obtained by the reaction at 250 °C under acid and base catalysts were lower than those for products generated in neutral hot-compressed water, as listed in Table 2-1. This is strong evidence suggesting that the catalyst-assisted hydrothermal treatment is still favorable for depolymerizing sodium alginate at high reaction temperatures (250 °C). However, the roles of catalysts for degrading sodium alginate seem to be gradually weakened as the reaction temperature increases.

2.3.2 Production of organic compounds

Based on the ^{1}H NMR and GPC data, alginate is converted to various organic compounds containing hydroxyl and carboxyl groups through the hydrolysis reaction [49, 51]. In HPLC analysis, the monomers and organic compounds produced by hydrothermal treatment at 150, 200 and 250 °C were observed as shown in Figure 2-6. Using a strong acid catalyst (pH 1) at 150 °C, the monomers were instantly generated as the reaction started. This indicates that the selective cleavage of glycosidic linkages was promoted by acid-catalyzed hydrolysis. The production of monomers was also observed in GPC data as shown in Figure 2-4-(a). The yield of monomers increased and then decreased within a few min with the production of furfural, glycolic acid and formic acid. This phenomenon was explained by the further decomposition of monomers through acid-catalyzed hydrolysis and dehydration. Another research group reported that mannuronic acid detaches from alginates faster than guluronic acid [50]. Similarly, the quantity of mannuronic acid was higher than that of guluronic acid in acidic and neutral aqueous reaction media at 150 °C in this study. It indicates that the acid catalyst does not influence the sequence of monomer dissociation in hot-compressed water, while it enhances the rate of production of each monomer in comparison with the catalyst-free hydrothermal depolymerization of alginate.

On the other hand, mannuronic acid and guluronic acid were not detected in the hydrothermal treatment of sodium alginate in the presence of a strong base catalyst (pH 13). Instead of monomers, carboxylic and dicarboxylic acids were produced more abundantly, with the amount increasing as reaction time increased. This suggests that a strong base catalyst substantially promotes the

decomposition of monomers via the Lorby de Bruyn–Alberta van Ekenstein Transformation (LBET), hydrolysis and dehydration reactions after the peeling reaction of alginate [49]. As a result, the monomers liberated from sodium alginate immediately converted into malic acid, fumaric acid, lactic acid, formic acid, etc., as shown in Figure 2-6-(a). The production of lactic and dicarboxylic acids was typical for a base-catalyzed hydrothermal decomposition of alginate or other hexuronic acids [49, 61]. In contrast to the strong acid and base catalysts, at 150 °C, weak acid (pH 3) and weak base (pH 11) catalysts did not show any remarkable difference in performance compared to the catalyst-free reaction (pH 7). The hydrothermal treatment of alginate in a pH range from 3 to 11 also produced monomers and organic acids, but it required at least 60 min to achieve that outcome.

The yield distribution of organic compounds produced at 200 °C is presented in Figure 2-6-(b). Monomers were almost consumed and the production of organic compounds was enhanced in comparison to the reaction at 150 °C. The production of formic acid, acetic acid and glycolic acid is common, and indicates that the reaction temperature (200 °C) is sufficiently high to decompose monomers into smaller organic acids regardless of the presence of an acid or base catalyst. Interestingly, the yield distribution of organic products shows clear differences between hydrothermal reactions under different pH conditions. The strong acid catalyst (pH 1) assisted the production of furfural, glycolic acid and small quantities of other organic acids. Compared with hydrothermal treatment at pH 1, the quantities of succinic acid increased, whereas the quantities of furfural and glycolic acid decreased in the pH range from 3 to 11. This implies that the production of furfural and glycolic acid is a unique feature of acid-catalyzed hydrothermal alginate decomposition. On the

other hand, malic acid, fumaric acid and lactic acid were generated under a strong base catalyst (pH 13), demonstrating that reaction pathways of monomer decomposition are strongly dependent upon the acidic or basic nature of the reaction solvents.

In the hydrothermal reactions of alginate at 250 °C, the overall yields of organic products for all pH conditions decreased as the reaction time increased. Such decrease indicates that thermally unstable compounds decomposed at 250 °C. For example, the yield of furfural decreased drastically under the strong acid catalyst (pH 1). This decrease was expected due to its low thermal stability in acidic aqueous media. To ensure the decomposition of furfural in this experimental system, the hydrothermal treatment of furfural in the acidic aqueous medium was performed with high-purity furfural (>99.0%). As expected, the conversion of furfural rapidly proceeded, resulting in the production of small amounts of organic acids and dark solid residues as shown in Figure 2-7. The solid residues are considered as humins formed by polymerization of furfural, known as “furfural resinification”, in the acidic hydrothermal conditions. These insoluble particles are observed when hexose or pentose are hydrothermally converted to furan compounds, such as 5-hydroxymethyl furfural or furfural [62, 63]. These insoluble particles were also generated in small quantities when alginate was hydrothermally treated in acidic reaction media. The production of humins is a major obstacle to produce furfural from the hydrothermal process, and the inhibition of humin production is important to enhance the yield of furfural.

As reaction temperatures increased from 200 to 250 °C at pH 13, yields of malic acid and fumaric acid also decreased as shown in Figure 2-6-(c). This indicates that these particular acids are unstable in the reaction condition. Those

two dicarboxylic acids were likely to convert into succinic acid and acetic acid at pH 13 at 250 °C, since it was observed that the yields of succinic acid and acetic acid increased as the reaction time increased. To clarify this, separate hydrothermal treatments of fumaric acid and malic acid was conducted at 250 °C at pH 13, as listed in Table 2-2. It was observed that malic acid and fumaric acid were consumed as the yields of succinic acid and acetic acid increased. It is believed that malic acid was rapidly transformed to fumaric acid by dehydration reaction and then fumaric acid produced converted to succinic acid and acetic acid. Although fumaric acid was hydrated to form malic acid, the dehydration of malic acid was likely to be more dominant in the reaction condition. To sum up, this high reaction temperature under the strong base catalyst decomposes both malic acid and fumaric acid, and depreciates the final product with the large amount of acetic acid. Therefore, either short reaction times at high temperatures or long reaction times at mild temperatures are favorable for production of hydrothermally unstable compounds, such as furfural, malic acid and fumaric acid. On the contrary, lactic acid was generated under all of the pH conditions at 250 °C without the decrease of yield, since the decomposition of lactic acid is feasible in near critical water (320–400 °C) [64]. The production of lactic acid was typical for the base-catalyzed hydrothermal depolymerization of alginate [49], and means that the high reaction temperature induced a base-catalyzed reaction by changing the properties of the hot-compressed water and promoting nucleophilic substitutions and elimination reactions. The high quantities of lactic acid at pH 13 at all of the reaction temperatures indicate that a strong base catalyst is very useful for the production of lactic acid via hydrothermal treatment of alginate in a wide range of temperature.

2.3.3 The effect of pH on product distribution

The distribution of organic products is strongly depending on the acid and base catalysts, as illustrated in Figure 2-8. The acid-catalyzed reaction promoted the production of furfural and glycolic acid, whereas the base-catalyzed reaction induced the production of lactic acid and dicarboxylic acids, such as malic acid and fumaric acid. Catalyst-free reaction at pH 7 showed poor performance in both alginate depolymerization and organic acid production. However, the performance was remarkably enhanced and all of the target products were detected at reaction temperatures higher than 200 °C. This indicates that the high reaction temperature induces both acid- and base-catalyzed hydrothermal reactions. Increasing reaction temperature influenced reaction pathways of hydrothermal conversion of alginate and changed the product distributions with the aid of catalysts. For example, lactic acid was produced under the strong acid catalyst at reaction temperatures higher than 200 °C, although it is a typical product from base-catalyzed hydrothermal decomposition of carbohydrate biomass including alginate [49, 52, 65]. Decomposition of furfural in the acidic hydrothermal condition is likely ascribed to the production of lactic acid at pH 1, as shown in Figure 2-6-(c) and Figure 2-7. This means that lactic acid can be produced by acid- or base-catalyzed hydrothermal decomposition of alginate at relatively high temperatures via totally different reaction pathways. In other words, in addition to the acid and base catalysts, the reaction temperature is an important factor determining the reaction pathways in hydrothermal conversion of alginate into organic compounds.

The hydrothermal treatment of cellulose was performed in identical reaction

conditions in order to analyze differences between cellulose and alginate in the aspect of the hydrothermal conversion of biomass-derived carbohydrates to valuable organic compounds. The cellulose was mechanically milled for over 20 h to enhance the susceptibility of crystalline cellulose to hydrothermal conversion, for effective conversion in hydrothermal conditions [66]. As shown in Table 2-3, a monomer of cellulose (glucose) also completely converted during hydrothermal treatment at pH 13, similar to the decomposition of mannuronic acid and guluronic acid with a strong base catalyst. In addition, monocarboxylic acids, such as lactic acid and formic acid, were obtained from the hydrothermal conversion of both cellulose and alginate. However, cellulose did not convert into dicarboxylic acids, such as malic acid, succinic acid or fumaric acid. At pH 1, glucose and furfural were produced significantly rather than organic acids. These differences likely arose from an extra carboxylic functional group in an alginate monomer. The acid-catalyzed degradation of cellulose showed better performance for production of furfural, compared with alginate. Most final products serve as useful platform chemicals in scientific and industrial fields [67]. Among those products, furfural, lactic acid and succinic acid were selected as important biomass-derived chemicals [68]. Prior to that, malic acid and fumaric acid were also ranked as top value-added chemicals from biomass in 2004, released by the US Department of Energy (DOE) [69]. In that respect, alginate has great potential as a promising renewable biomass feedstock for production of furfural and value-added organic acids.

Table 2-1 Weight average molecular weight (Mw), number average molecular weight (Mn) and polydispersity index (PDI) values of raw alginate and hydrothermally-treated alginate under different reaction conditions.

Raw alginate	Reaction time	M_w (Da)	M_n (Da)	PDI
Sample		277865	65185	4.26
pH 1 – 150 °C	0 min	9453	1269	7.45
	6 min	4159	1039	4
	15 min	1396	841	1.66
	60 min	1710	819	2.09
pH 7 – 150 °C	0 min	268446	107320	2.5
	6 min	129806	50913	2.55
	15 min	36506	15440	2.36
	60 min	3608	1870	1.93
pH 13 – 150 °C	0 min	704	533	1.32
	6 min	683	521	1.31
	15 min	711	537	1.33
	60 min	699	519	1.35
pH 1 – 250 °C	0 min	873	703	1.24
	6 min	817	679	1.2
	15 min	753	650	1.16
	60 min	693	607	1.14
pH 7 – 250 °C	0 min	1367	1009	1.35
	6 min	1171	905	1.29
	15 min	1251	994	1.26
	60 min	1247	962	1.30
pH 13 – 250 °C	0 min	682	535	1.27
	6 min	678	533	1.27
	15 min	649	524	1.24
	60 min	646	519	1.25

Table 2-2 Conversion and yields of organic acid products obtained from hydrothermal treatment of dicarboxylic acids at 250 °C and pH 13.

	Starting Material (2 wt% in 3 mL of H_2O)					
	Malic acid			Fumaric acid		
Reaction time (min)	3	15	30	3	15	30
Conversion (%)	63	90.6	93.6	8.8	66.4	90.9
Compound	**Yield (mol%)**					
Formic acid	0	0	0	0	0	0
Acetic acid	9.2	45.6	88.3	10.7	60.1	82.7
Glycolic acid	0.5	0.2	0.5	0.5	0.9	0.3
Lactic acid	0.1	0.3	0.4	0	0.4	0.8
Succinic acid	0.7	9.2	11.7	1.1	5.4	11.4
Fumaric acid	91.9	23	14.2	-	-	-
Malic acid	-	-	-	35.6	17.0	5.4

Table 2-3 Yields of organic compounds produced by hydrothermal treatment of sodium alginate and cellulose at 150 °C for 30 min in the presence of strong acid or base catalysts.

Product	Yield (mol%)			
	pH 1		pH 13	
	Alginate	Cellulose	Alginate	Cellulose
Monomer	4.3	6.6	0.0	0.0
Furfural	1.7	3.3	0.0	0.0
Malic acid	0.0	0.0	3.1	0.0
Succinic acid	0.0	0.0	0.4	0.0
Glycolic acid	2.5	0.0	0.6	0.2
Fumaric acid	0.0	0.0	2.8	0.0
Lactic acid	0.0	0.0	3.5	4.8
Acetic acid	0.5	0.6	4.9	0.0
Formic acid	0.0	0.9	1.1	2.8
Total	9.0	13.2	16.4	7.8

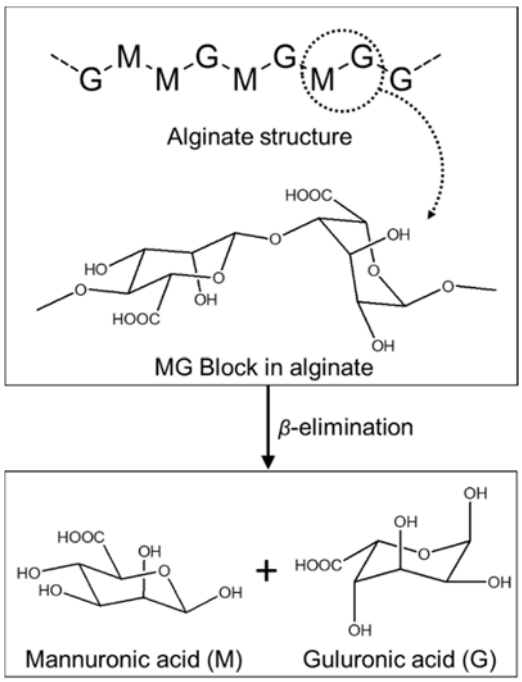

Figure 2-1. Decomposition of alginate via the cleavage of 1, 4-glycosidic linkages in a β-elimination pathway.

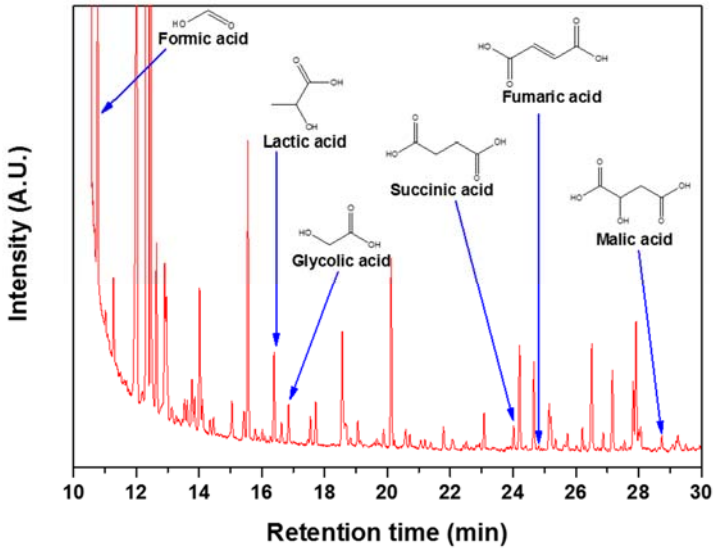

Figure 2-2. GC-MS chromatogram of organic compounds obtained after hydrothermal treatment of sodium alginate at pH 7 and 200 °C for 60 min.

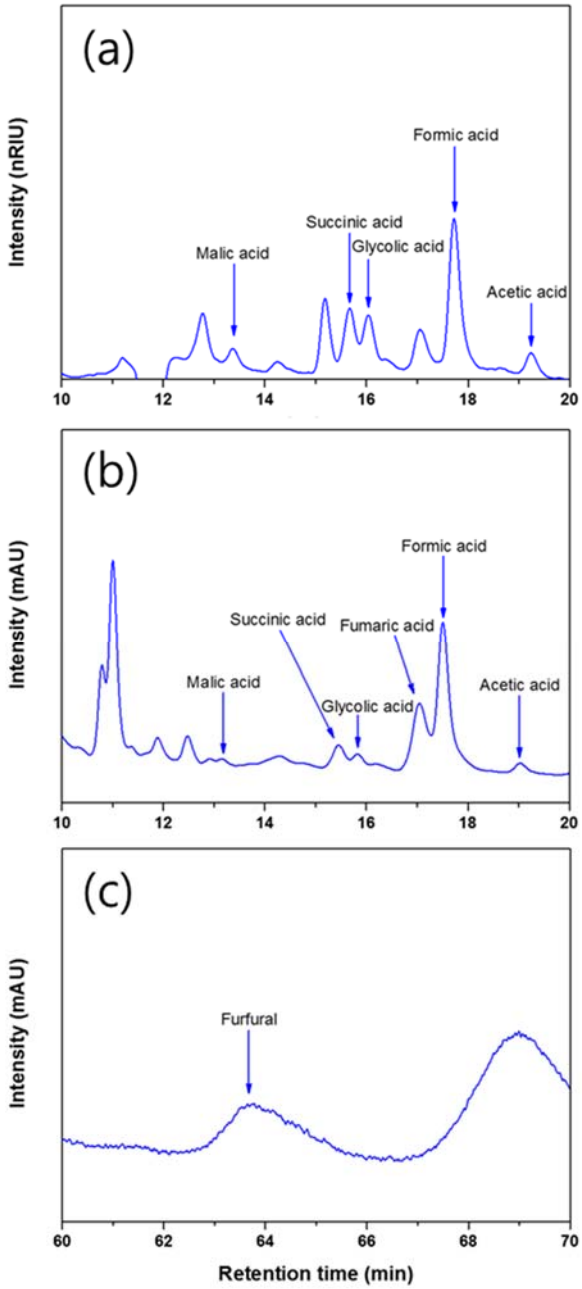

Figure 2-3. HPLC chromatograms of organic compounds produced via hydrothermal treatment of sodium alginate at pH 7 and 200 °C for 60 min. (a) HPLC-RID, (b) and (c) HPLC-VWD.

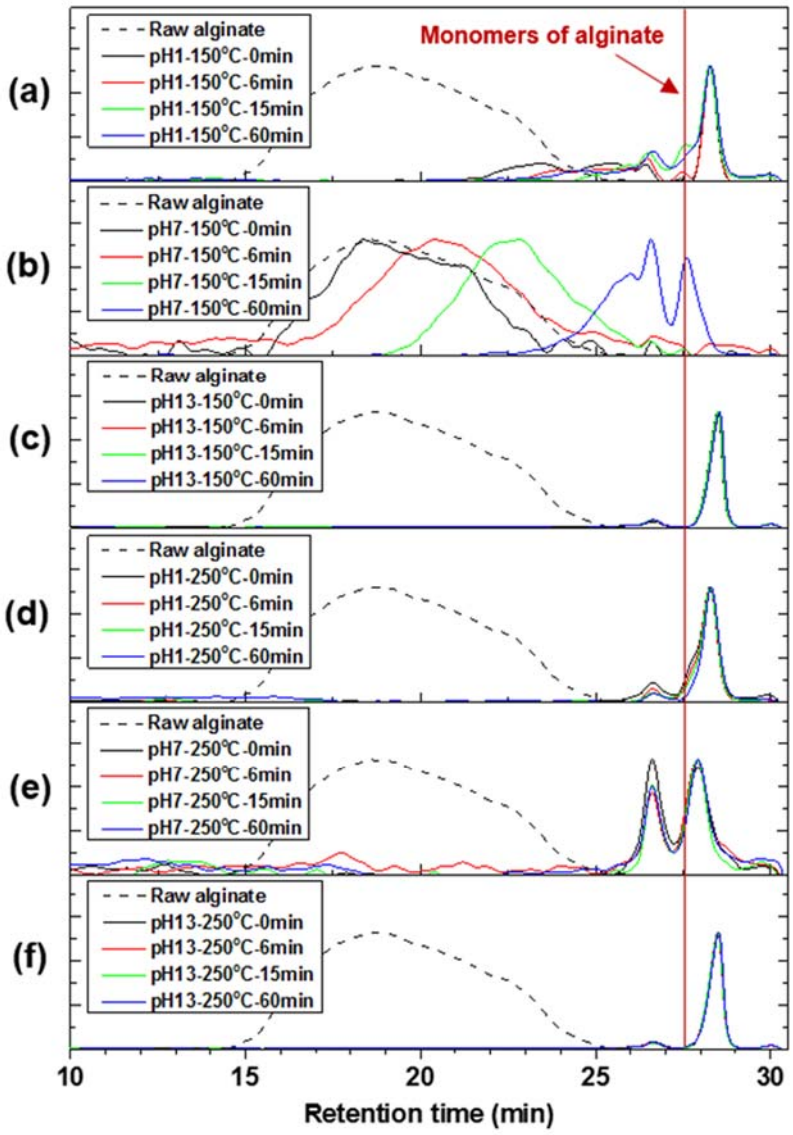

Figure 2-4. GPC chromatograms of raw alginate and products obtained by hydrothermal depolymerization of raw alginate: (a) pH 1, 150 °C, (b) pH 7, 150 °C, (c) pH 13, 150 °C, (d) pH 1, 250 °C, (e) pH 7, 250 °C, (f) pH 13, 250 °C.

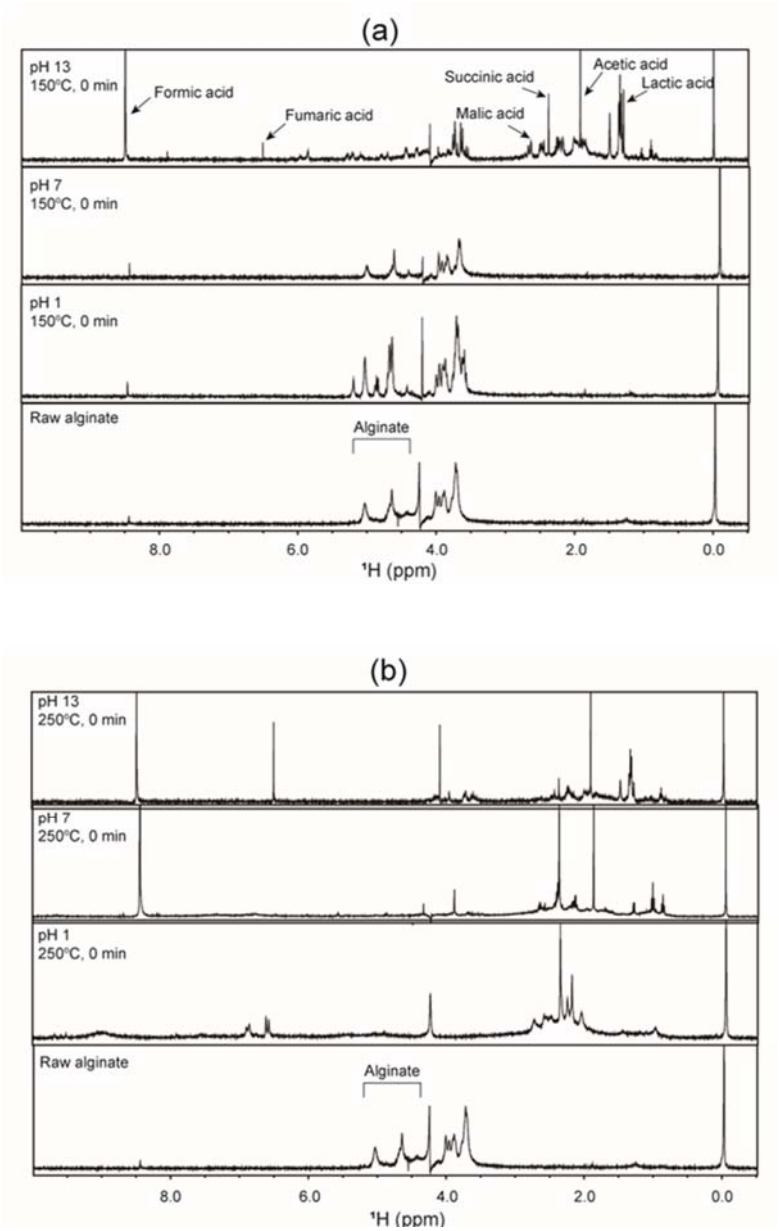

Figure 2-5. ^{1}H NMR spectra of raw alginate and hydrothermally treated alginate solutions; H-1 of guluronic acid (δ = 4.95~5.17), H-5 of guluronic acid and H-1 of mannuronic acid (δ = 4.55~4.82), H-5 of guluronic acid (δ = 4.40~4.50).

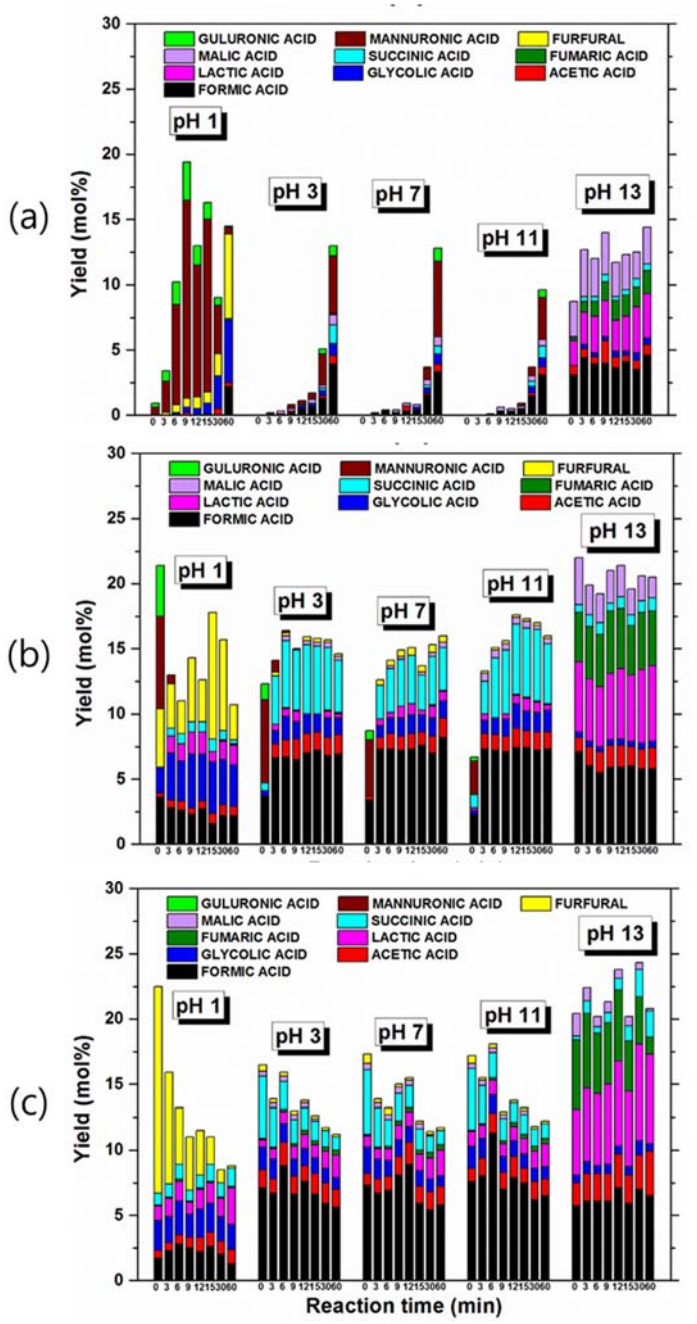

Figure 2-6. Molar yields of monomers and organic acids produced by hydrothermal decomposition. (a) 150 °C, (b) 200 °C, (c) 250 °C. Reaction times marked beneath each column are as follows: 0, 3, 6, 9, 12, 15, 30 and 60 min.

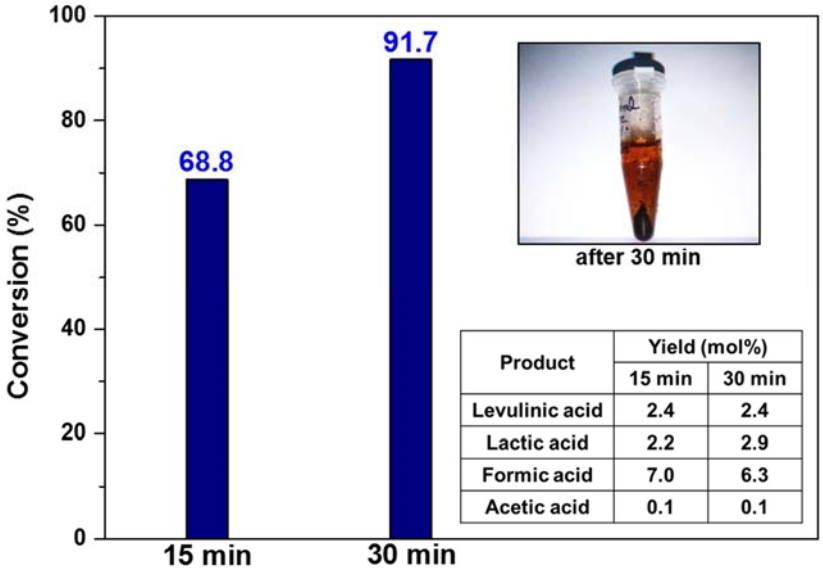

Product	Yield (mol%)	
	15 min	30 min
Levulinic acid	2.4	2.4
Lactic acid	2.2	2.9
Formic acid	7.0	6.3
Acetic acid	0.1	0.1

Figure 2-7. Conversion of furfural and yields of products after hydrothermal treatment of furfural at pH 1 and 250°C.

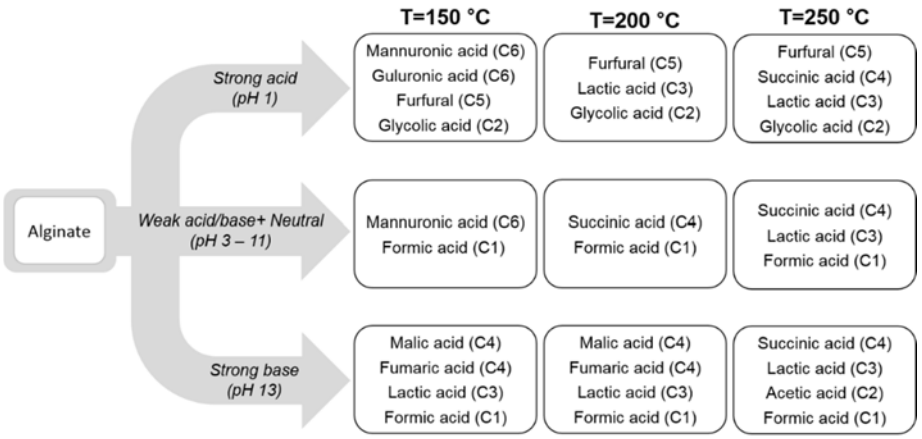

Figure 2-8. Effect of initial pH of aqueous medium and reaction temperature on product distribution.

Chapter 3. Catalytic Hydrothermal Conversion of Alginate to Lactic Acid over Metal Oxides

3.1 Introduction

Hydrothermal process for production of high value-added organic compounds from biomass-derived carbohydrates is an inexpensive and environmentally benign method, since water is used as a reaction medium acting as a catalyst in hydrothermal conditions [27]. The aqueous medium in the hydrothermal conditions has a larger ion product ($K_w=[H^+][OH^-]$) and smaller relative dielectric permittivity than water at room temperature, which induces the hydrothermal reaction of carbohydrates [26]. In the subcritical water system, various homogeneous and heterogeneous catalysts can be employed to catalyze the hydrothermal reaction and enhance the yields and selectivities of target products. Among many target products, lactic acid has been in the limelight due to its broad applicability in various industrial fields. In the chemical industry, lactic acid has great potential as a platform chemical for the production of pyruvic acid, propylene glycol, acrylic acid, acetaldehyde and lactides [70-72]. Additionally, lactic acid has wide applications for alternative fuels, food commodities, pharmaceutical products, biodegradable polymers and eco-friendly solvents [67, 73, 74]. Lactic acid production has been achieved via catalytic hydrothermal treatment of lignocellulosic biomass feedstock under various homogeneous and heterogeneous catalysts [52, 65, 75-77]. However, there are only a few studies that use alginates as a carbohydrate feedstock for the production of lactic acid. In the 1960s, hydrothermal treatment of alginate was conducted at different pH values under mild temperatures, but these studies

were focused on the physical properties of depolymerised alginate, not on the production of organic acids [22, 58, 59]. Whistler and BeMiller reported the formation of 6-carbon organic acids via alkaline depolymerization of alginates at 80–120 °C [78]. However, further studies on the hydrothermal conversion of 6-carbon compounds to light organic acids were not performed. In 1985, Niemela and Sjostrom studied the hydrothermal conversion of alginate to various mono- and di-carboxylic acids under NaOH and $Ca(OH)_2$ at 95 °C and 135 °C [49]. Lactic acid was the main mono-carboxylic acid produced by the alkaline hydrothermal reaction, indicating that alginate can be utilized as a carbohydrate source for the production of lactic acid. In previous work introduced in Chapter 2, it was found that the production of lactic acid was promoted by adding NaOH to the reaction solvent in the temperature range of 150–200 °C [79]. However, the usage of strong alkaline solutions as the reaction media causes time-consuming and costly separation of catalysts from homogeneous product mixtures, in addition to reactor corrosion by alkaline hot-compressed water.

In this work, the catalytic hydrothermal conversion of alginate to lactic acid was investigated with using Al_2O_3, MgO, Mg-Al mixed oxides, CaO, ZnO, ZrO_2, CeO_2 and TiO_2 as a solid base catalyst. The effects of experimental parameters, such as reaction temperature, reaction time and the amount of catalyst loading, on the yield of lactic acid were investigated. The catalytic performance of the metal oxide catalysts in the depolymerization of alginate and production of lactic acid was evaluated based on catalyst characterization and product analysis. The relation between the basicity of catalysts and catalytic performance is mainly discussed. In addition, plausible reaction pathways from alginate to lactic acid and α-hydroxyglutaric acid are suggested.

3.2 Experimental

3.2.1 Preparation of metal oxide catalysts

Sodium alginate, α-hydroxyglutaric acid (>95%), lactic acid, acetic acid (>99%), formic acid (>95%), sodium hydroxide (>98%), pyruvaldehyde (40 wt% in H_2O), D-(+)-glyceraldehyde (>98%), dihydroxyacetone dimer (>97%), pH indicator (phenolphthalein, 0.5 wt% in ethanol: water (1:1)) and derivatization agent (BSTFA+TMCS, 99:1) were purchased from Sigma-Aldrich. Monomers of alginate (>98%), mannuronic acid and guluronic acid, were obtained from Qingdao BZ Oligo Biotech. Glucuronic acid (>98%) was obtained from Alfa Aesar. Calcium oxide was prepared by the calcination of calcium hydroxide (>95%, Sigma-Aldrich) at 800 °C for 5 h. Magnesium oxide was obtained by the calcination of magnesium hydroxide (>95%, Sigma-Aldrich) at 600 °C for 2 h. Other catalysts were prepared by thermal treatment of commercial metal oxides: aluminum oxide (Sasol, 550 °C, 2 h), $Mg_{30}Al_{70}$ (Sasol, 800 °C, 6 h), hydrotalcite (Sigma-Aldrich, 800 °C, 6 h), zinc oxide (Sigma-Aldrich, 600 °C, 3 h), zirconium oxide (Sigma-Aldrich, 600 °C, 3 h), titanium oxide (Sigma-Aldrich, 500 °C, 2 h) and cerium oxide (Rhodia, 500 °C, 2 h). The crystal structure of metal oxides was visualized by X-ray diffraction analysis as shown in Figure 3-1.

3.2.2 Reaction procedure

Sodium alginate was hydrothermally treated in various reaction conditions using a stainless steel batch reactor (50 mL) lined with Teflon. It was believed

that the effective heterogeneous reaction was achieved without mass transfer limitations, since a stirrer located inside the reactor (diameter of impeller = 2.8 cm) rotated at 600 rpm, inducing a fully turbulent mixing flow (Reynolds number ≈ 7800). Sodium alginate (0.6 g) and solid catalysts (0.6g) were added to the distilled water (30 mL) in the reactor. After sealing the reactor, the inside of the reactor was purged with nitrogen gas and the reactor was mounted in a heater. As shown in Figure 3-2, the elapsed time to reach a target temperature (120, 140, 160, 180, 200 and 220 °C) was measured and the time was excluded in defining reaction time. After the reaction was completed at the target temperature, the reactor was immediately immersed in a cold-water bath. It was presumed that the aqueous solvent exists as saturated water in these reaction conditions, based on water properties calculated with the equation of state. Prior to product analysis, product mixtures were centrifuged and diluted. Separated catalysts after the reaction were washed with distilled water and ethanol, followed by drying overnight in an oven at 105 °C. Deactivated catalysts were regenerated by thermal treatment in the calcination conditions.

3.2.3 Characterization of catalysts

The surface areas of the prepared catalysts were measured via a nitrogen adsorption-desorption method based on a Brunauer-Emmett-Teller (BET) model with a physisorption analyzer (ASAP 2010, Micromeritics). Pretreatment of samples was performed at 100 °C for 3 h under vacuum and sorption was achieved with liquid nitrogen.

The crystal structures of catalysts were analyzed by a X-ray diffractometer (SmartLab®, Rigaku) with Cu Kα radiation (λ=0.154 nm) at 40 kV and 30 mA

between 10 to 80° of 2 theta. The analysis of XRD patterns was carried out using the Joint Committee of Powder Diffraction Standards database (JCPDS).

In order to analyze the basic property of metal oxides, temperature-programmed desorption of CO_2 was executed with a catalyst analyzer (BELCAT, BEL JAPAN INC.) equipped with a TCD detector. The adsorption of CO_2 on the catalysts was performed at 50 °C for 1 h after pretreatment at temperatures 50 °C lower than the calcination temperature of each catalyst under helium flow. The desorption of CO_2 adsorbed on the catalysts was achieved by increasing the furnace temperature from 50 °C to the target temperatures at a ramping rate of 10 °C min^{-1}, followed by holding at the final temperatures for 1 hr.

Quantification of Brønsted basicity was conducted by titration using oxalic acid and phenolphthalein aqueous solution containing ethanol. The prepared catalysts were added to distilled water and the mixtures were vigorously stirred for 1 h, followed by separating the catalysts from the mixtures and adding phenolphthalein solution to the solid-free mixtures. The hydrochloric acid (0.05 M) was added dropwise to the mixtures with shaking until the pink color of the mixtures disappeared. The basicity was calculated by dividing the amount of consumed hydrochloric acid by the mass of catalyst used.

3.2.4 Product analysis

After all reactions were completed, used solid catalysts were separated from liquid products by filtration and centrifugation. Product was identified with a GC-MS System (Clarus 680/600T, Perkin-Elmer) equipped with an Agilent DB-5MS column. For GC-MS analysis of the organic acids, water soluble

products were lyophilized and silylated with a mixture of BSFTA with TMCS (99:1) and pyridine at 65 °C for 2 h. As a result, lactic acid, α-hydroxyglutaric acid, glycolic acid, 2-hydroxybutyric acid and dihydroxyacetone were detected for a sample obtained by hydrothermal treatment of alginate at 200 °C for 1 h, as shown in a GC-MS spectrum of Figure 3-3.

The liquid products were identified using a LC-MS system (Surveyor, Thermo Finnigan) in combination with a mass spectrometer (LCQ Deca XP Plus, Thermo Finnigan) equipped with an electrospray ionization module and working in negative mode ($[M-H]^-$ or $[M-Na]^-$) with a capillary temperature of 275 °C. Three types of mobile phases (0.1% of formic acid dissolved in distilled water, acetonitrile or methanol) were delivered to a column (Synergi™ 4 μm Polar-RP 80 Å, LC Column 150 x 2 mm, Phenomenex) at a flow rate of 0.25 mL min^{-1}. The UV wavelength was set as 214, 254 and 280 nm.

The final products were quantified with an Agilent 1200 Series HPLC equipped with two Shodex RSpak KC-811 columns in series. Phosphoric acid aqueous solution (5 mM) was run through the column (40 °C) at a flow rate of 1.0 mL min^{-1}. RI detector (Agilent G1362A) and UV detector (Agilent G1314B) were used together for more precise analysis. The wavelength of the UV detector was set to 210 nm.

3.3 Results and discussion

3.3.1 Catalytic effects of metal oxide catalysts on lactic acid yield

The hydrothermal treatment of sodium alginate over metal oxides yielded carboxylic and dicarboxylic acids as listed in Table 3-1. The surface area and density of the basic sites of catalysts were also measured to investigate the relationship between the yields and catalyst properties. Herein, the basic site was divided into three temperature regions, such as strong (T>500 °C), medium (300<T<500 °C) and weak (T<300 °C), based on CO_2 desorption temperatures. Gaussian functions were used to deconvolute a few CO_2-TPD patterns showing broad and overlapped peaks as illustrated in Figure 3-4. In the catalyst-free reaction, the yields of lactic acid and α-hydroxyglutaric acid were 0.74% and 0.88%, respectively. These two organic acids are mainly produced during alkaline hydrothermal decomposition of alginate [49], which means that the base-catalyzed reaction for the production of lactic acid and α-hydroxyglutaric acid was not activated in the absence of catalysts. Formic acid was constantly produced in all of the reactions, with small amounts of glycolic acid and acetic acid. CaO exhibited the highest lactic acid yield despite its small surface area (8.7 $m^2 g^{-1}$), demonstrating that surface area was not an important factor determining catalytic activity.

As shown in the profile of CO_2 adsorption in Figure 3-4-(e), CaO catalyst has three CO_2-TPD peaks near 110, 320 and 560 °C. A moderate density of weak basic sites (2.66×10^{-3} mmol m^{-2}) was observed on CaO. The density of medium basic sites was 1.61×10^{-2} mmol m^{-2}, a few orders

of magnitude larger than other catalysts. It was interesting to note that only the CaO catalyst possessed a high density of strong basic sites. The relatively large densities of medium and strong basic sites on the CaO catalyst likely promoted the base-catalyzed reaction to produce lactic acid. However, Liu et al. suggested that the CaO catalyst is inactive during the hydrothermal conversion of glucose to methyl lactate at 200 °C because the catalyst has only strong basic sites with a remarkably higher concentration than those of ZrO_2 and MgO catalysts [80]. These strong basic sites, dominantly composed of isolated O^{2-} ions in metal oxides, is associated with the unidentate carbonate formed by CO_2 adsorption on the catalysts, which hinders from forming ethoxide intermediate by the dissociative adsorption of ethanol [81]. The strong basic sites would impede the dissociative adsorption of water molecules, producing Brønsted base (OH^-) in the hydrothermal reaction of alginate, with negative effects on the production of lactic acid. On the other hand, the medium basic sites associated with Ca^{2+}-O^{2-} pairs produce bidentate carbonate during CO_2 adsorption, which indicates that these sites are favorable for producing Brønsted base via the dissociative adsorption of water on the Lewis acid-strong base pair sites. It was reported that ethanol dissociates to ethoxide ions and protons following interaction with Mg^{2+}-O^{2-} pairs in the dehydration of ethanol to acetaldehyde [81]. In other words, the highest lactic acid yield obtained by the base-catalyzed reaction can be related to the highest density of medium basic sites on the CaO catalyst. Based on the correlation between previous studies and current experimental data, the medium basic sites on CaO seem to act as active sites for the hydrothermal conversion of alginate to lactic acid.

On the other hand, Al_2O_3 exhibited low catalytic activity in the production of lactic acid in spite of its largest surface area. This can be explained by the fact that the smallest amount of CO_2 was desorbed from Al_2O_3. On the other hand, the addition of MgO into Al_2O_3 as Mg-Al mixed oxides enhanced the yields of lactic acid and α-hydroxyglutaric acid, increasing the density of basic sites. This indicates that the higher MgO content induced the increment of basic active sites in the Mg-Al mixed oxide system due to its basic nature [82]. Compared to hydrotalcite, pure MgO yielded a smaller amount of lactic acid although MgO possesses approximately 5 times the amount of weak basic sites and 10 times the amount of strong basic sites. α-hydroxyglutaric acid was primarily produced when MgO was used in the hydrothermal decomposition of alginate. This result suggests that the MgO catalyst was favorable for yielding α-hydroxyglutaric acid instead of lactic acid. The other catalysts, ZnO, ZrO_2 and TiO_2, showed low catalytic performance similar to the catalyst-free reaction despite the considerable densities of weak basic sites compared to CaO. CO_2 adsorbs onto weak basic sites, forming bicarbonate with the surface hydroxyl groups of the catalysts, which implies that the dissociative adsorption of water is rare [81]. That is rationalized by the fact that the densities of weak basic sites on the catalysts may have little influence on the yield of lactic acid. In addition, the densities of medium basic sites on ZnO, ZrO_2 and CeO_2 could not be associated with the lactic acid yield, implying that the structure of medium basic sites is dissimilar to that of CaO (Ca^{2+}-O^{2-} pairs) due to a difference between their crystal structures and the octahedral structure of CaO. For this reason, the densities of basic sites determined by CO_2-TPD

cannot be directly associated with the catalytic activities of various catalysts in hydrothermal reactions. Moreover, the basicity was measured in the gas phase instead of an aqueous medium, causing the inconsistency between the CO_2-TPD profile and the catalytic activity.

To scrutinize the relationship between the basic property of metal oxides and the lactic acid yield, the catalysts were titrated with oxalic acid in order to measure the number of Brønsted base (OH^-) accessible to reactants in an aqueous medium. As shown in Figure 3-5, the lactic acid yield was strongly dependent on the amount of Brønsted base released from the catalyst. CaO, possessing the largest basicity (4.72 mmol g^{-1}), showed the highest lactic acid yield of 12.66%. This corresponds well with the results of CO_2-TPD analysis as shown in Table 3-1. Similar to the CO_2-TPD result, the mixed metal oxides including MgO showed higher basicity than pure Al_2O_3 in the aqueous reaction medium. The enhanced production of lactic acid can be explained by the fact that the active catalysts such as CaO, MgO and Mg-Al mixed oxides, releases OH^- ions into the aqueous reaction medium via the dissociative adsorption of water molecules onto the catalysts' surfaces [81, 83]. The Brønsted base in the aqueous phase promotes the base-catalyzed reaction, producing lactic acid via retro-aldol condensation and dehydration. Onda et al. reported that the larger amount of Brønsted base obtained at higher calcination temperatures promoted the production of lactic acid by hydrothermal treatment of glucose under hydrotalcite [84]. Recently, Choudhary et al. also reported a linear correlation between the basicity measured by titration and lactic acid yield in hydrothermal decomposition of glucose over magnesia-supported calcium catalysts [85]. Based on

previous research introduced in Chapter 2, the Brønsted base can play a role of catalyst for the production of lactic acid in the hydrothermal reaction of alginate. However, the production of α-hydroxyglutaric acid was not significantly influenced by the amount of Brønsted base as shown in Figure 3-6. For example, the yield of α-hydroxyglutaric acid over CaO was lower than that over MgO despite of the largest basicity of CaO, which suggests that the CaO catalyst is favorable for the production of lactic acid rather than α-hydroxyglutaric acid. On the other hand, the inactive catalysts in the production of lactic acid, such as Al_2O_3, ZnO, ZrO_2 and TiO_2, could not be titrated due to the lack of color variation for the phenolphthalein indicator, suggesting that there were few or no Brønsted base sites from those catalysts. This result presents clear evidence explaining the low lactic acid yields of less than 1% obtained by hydrothermal treatment of alginate using those four metal oxides. In addition, based on the results of titration and CO_2-TPD, it was obvious that the considerable densities of weak and medium basic sites on ZnO, ZrO_2 and TiO_2 did not contribute to the generation of Brønsted base (OH^-) to enhance the production of lactic acid. Therefore, the basic property of metal oxide catalysts measured by the titration method seems more reasonable than by the CO_2-TPD method for hydrothermal reaction of alginate.

3.3.2 Influence of experimental conditions on production of organic acids

The effects of reaction conditions on the catalytic performance of CaO in the hydrothermal reaction of alginate was studied with varying reaction

temperature, time and catalyst loading. Figure 3-7-(a) shows the effect of reaction temperature on the production of α-hydroxyglutaric acid, lactic acid, glycolic acid, acetic acid and formic acid. At 120 °C, the yield of formic acid was highest among the products. As the reaction temperature was increased to 160 °C, the amount of lactic acid produced tripled compared to the amount at 120 °C and the formic acid yield reached a maximum value of 9.15%. At temperatures above 160 °C, the production of lactic acid was still enhanced while the formic acid yield decreased. The yields for other organic products, such as α-hydroxyglutaric acid, glycolic acid and acetic acid, slightly increased as the reaction temperature increased. The overall increase in organic acid yields can be explained by the fact that the larger thermal energy induced by increasing the reaction temperature accelerated the dissociation of water molecules to H^+ and OH^- ions, which promoted the acid- and base-catalyzed reaction, respectively. In addition to the catalytic effect of increasing the ion product, CaO further accelerated the base-catalyzed reaction, yielding lactic acid and α-hydroxyglutaric acid by providing Brønsted base (OH^-) into the aqueous reaction medium as the reaction temperature increased. Figure 3-7-(b) shows the variation in product distributions obtained from the sodium alginate reaction over the CaO catalyst at different reaction times. After 1 h, the yields of lactic acid, formic acid and α-hydroxyglutaric acid were 12.66%, 7.60% and 3.84%, respectively. These yields remained almost the same after further reaction for up to 12 h, implying that the catalyst hardly deactivated. The maximum yields of lactic acid and formic acid were 14.66% and 9.77%, respectively, at 6 h and those values gradually decreased as the reaction progressed beyond 6 h. More than 85 percent of the maximum amount of lactic acid was produced during the first hour of the reaction, indicating that the CaO

catalyst shows good catalytic performance within a short reaction time. The amount of catalyst added to the hydrothermal reaction significantly influenced the production of organic acids as shown in Figure 3-7-(c). The lactic acid yield increased linearly as the amount of catalyst was increased from 0 to 600mg. Catalyst loading above 600 mg was not effective for the production of lactic acid. The yield of α-hydroxyglutaric acid increased with increasing catalyst loading, however, it began to decrease when the catalyst loading exceeded 150 mg. On the other hand, the glycolic acid yield decreased with increasing catalyst loading, suggesting that the increase in Brønsted base by adding the CaO catalyst suppressed the acid-catalyzed reaction, which produces glycolic acid from sodium alginate [79]. That is, the abundant amount of OH^- ions released from the CaO catalyst counterbalanced Brønsted acids, H^+ ions, in the hot-compressed water, promoting the production of lactic acid and α-hydroxyglutaric acid instead of glycolic acid. The almost constant yields of formic acid and acetic acid imply that the production of formic acid and acetic acid was not hardly influenced by the concentration of Brønsted base in the hydrothermal conditions.

3.3.3. Catalytic performance of CaO

The catalytic activities of heterogeneous and homogeneous catalysts were compared based on the yields of organic acids mainly produced by the hydrothermal conversion of alginate. For comparison, MgO and NaOH were selected as representative basic catalysts in hydrothermal biomass conversion for the production of lactic acid or its derivatives [76, 80]. The yield of lactic acid over MgO was 3.36%, almost half of that obtained over NaOH. However,

the lactic acid yield obtained from the hydrothermal reaction over CaO, 12.66%, was about 2 times higher than with NaOH (0.5M), 6.61%. Although the concentration of NaOH was doubled, the lactic acid yield was less than half of that over CaO. On the other hand, the yields for all other organic acids produced from the hydrothermal reaction over NaOH were higher than those over CaO. This suggests that the reaction pathways of the base-catalyzed hydrothermal reaction vary according to whether the reaction is catalyzed by heterogeneous or homogeneous catalysts. Based on the results, CaO showed better catalytic performance for the production of lactic acid than NaOH. The yields of organic acids were almost constant during long-term reactions as shown in Figure 3-9.

The CaO catalyst showing the best catalytic performance in the production of lactic acid is transformed to $Ca(OH)_2$ in the aqueous reaction medium, as shown in Figure 3-10. The transformation seems to contribute to the higher basicity of CaO compared to other metal oxides. Base on the XRD patterns, $Ca(OH)_2$ is likely an actual catalyst in the hydrothermal reaction of alginate. To check the expectation, only $Ca(OH)_2$ was used as a catalyst in the hydrothermal reaction at 200 °C for 1 h. Based on the assumption that CaO is completely transformed to $Ca(OH)_2$, the same mole of $Ca(OH)_2$ was used in the reaction. As a result, the yield of lactic acid obtained by the catalytic conversion of alginate over $Ca(OH)_2$ is 6.9% lower than over CaO (12.66%). The lower catalytic activity of $Ca(OH)_2$ than CaO can be explained as that $Ca(OH)_2$ easily releases hydroxyl ions but it cannot catalyze the dissociation of water molecules. Based on the activity tests of CaO and $Ca(OH)_2$, the CaO catalyst is not completely transformed to $Ca(OH)_2$ and still plays a role of base catalyst in the hydrothermal reaction of alginate.

Heterogeneous catalysts can be easily separated from aqueous product

mixtures and recycled after posttreatments like washing and drying. The reusability of the CaO catalyst was evaluated as shown in Figure 3-11. In the first experiment that lasted at 200 °C for 1 h, the yields of lactic acid, α-hydroxyglutaric acid and formic acid, were 12.14, 3.54 and 7.35%, respectively. After simple cleaning and drying, the used catalyst was re-applied to the hydrothermal reaction of sodium alginate with the same conditions. In the second run, the yields of organic products were almost the same as those in the first run. However, the catalytic activity was attenuated in the third run, indicating that the CaO catalyst can be reused once without the loss of catalytic performance. In the 3rd reaction, the glycolic acid yield increased whereas the amount of lactic acid decreased by half. This suggests that the Brønsted base on CaO were almost depleted by the repeated hydrothermal reactions of alginate while the acid-catalyzed reaction was revived by the Brønsted acids provided by the hot-compressed water. To regenerate the catalytic activity of the CaO catalyst, the used catalyst was re-calcined at 800 °C for 5 h under ambient conditions. After the simple thermal treatment, the original catalytic performance of the CaO catalyst was successfully recovered and the lactic acid yield increased from 5.01 to 12.63%. In the same manner, the regenerated CaO catalyst was also deactivated after two repeated reactions with a decrease in lactic acid yield from 12.69 to 3.59%. The regenerated catalytic activity can be attributed to the recovery of basicity (2.78 mmol g^{-1}) measured by titration. The recovery of basicity indicates that the recalcination of the deactivated CaO catalyst successfully regenerates the Brønsted basic site on the CaO catalyst.

In general, solid catalysts are deactivated after heterogeneous reactions in liquid phases, related to the adsorption of byproducts onto the catalyst surface, collapse of the catalyst structure or leaching of active sites [86, 87]. In the

reaction conditions, the byproduct adsorption seemed dominant, since the weights of used catalysts slightly increased with color variations of the used catalysts. The color of the CaO catalyst gradually changed from white to the color of the liquid product, dark brown, as the catalytic hydrothermal reaction was repeated. The byproducts seem to be alginate-derived organic compounds, such as oligomers and acids, which may cover the active sites of the CaO catalyst. After the third run, the color of the used catalyst was almost similar to that of the liquid product, which implies that the byproducts in the liquid product blocked the Ca^{2+}-O^{2-} pair sites. As evidence, it was observed that the twice-used CaO catalyst did not provide Brønsted base in the titration test. In addition, as presented in Table 3-2, the small amounts of organic acids were detected during the hydrothermal treatment of the used CaO catalyst in the absence of sodium alginate in the same reaction conditions after sufficient washing of the used catalyst, indicating the adsorbed organic compounds hydrothermally converted to organic acids such as lactic acid by the base-catalyzed reaction. Based on the results, the deactivation of the CaO catalyst seems to be more dependent on the alginate-derived byproducts covering the active sites on the CaO catalyst than the hydrothermal conditions itself. For example, if the severity of hydrothermal conditions caused the deactivation of the CaO catalyst, the lactic acid yield at the third run should be much lower than 11.95%, as shown in Figure 3-11. The organic byproducts were likely removed by the recalcination, which was evidenced by observation that the dark color of the deactivated catalyst was restored to white and the basicity increased from almost zero to 2.78 mmol g^{-1}. In addition to the recovery of basicity in the aqueous phase, weak, medium and strong basic sites were also recovered after the regeneration process as shown in Figure 3-12. The amount of CO_2 desorbed

from the regenerated CaO catalyst decreased by approximately 3 times compared to that of the fresh CaO catalyst, although the lactic acid yield more than doubled after the catalyst regeneration. This implies that the decreased density of active sites, specifically medium basic sites, was sufficient to promote the dissociative adsorption of water molecules.

3.3.4 Effect of metal oxides on depolymerization of alginate

The effect of different metal oxides on the depolymerization of alginate was elucidated by GPC analysis. The degradation of raw alginate was clearly observed and all chromatograms converged into a camelback-like shape between 24 and 30 min, as plotted in Figure 3-13. The longer retention time on the GPC chromatograms indicates the existence of smaller molecules in the products. It was observed that there were two groups of products with larger or smaller molecular weights than the monomers of alginate. For more detailed comparison of catalytic performance in the decomposition of alginate, the weight average molecular weight (M_w), the number average molecular weight (M_n) and the polydispersity index (PDI) were calculated based on the GPC data, as listed in Table 3-3. In spite of the absence of catalysts, the molecular weights of raw alginate were reduced drastically at 200 °C for 1 h with a decrease in PDI value from 4.26 to 1.59. This result indicates that the reaction temperature and time were sufficient to depolymerise the alginate with the production of smaller molecules possessing narrow molecular weight distributions. The catalyst-aided reactions induced smaller M_w and M_n than the catalyst-free reaction, which implies that the addition of metal oxides as catalysts promoted alginate depolymerization. However, the hydrothermally treated alginate over

ZnO had larger molecular weights than that of the blank test. To further investigate the catalytic effect on the hydrothermal depolymerization of alginate in detail, molecular distribution curves were plotted as shown in Figure 3-14. Hydrothermal reactions with no catalyst as well as those with CaO and ZnO were also analyzed to compare the catalytic performance in alginate degradation. On the camelback-like chromatograms, the left and right peaks indicate the production of molecules smaller and larger than monomers, respectively. As shown in the ZnO chromatogram, the right peak was larger than the left, indicating that molecules larger than monomers were more abundant. A shoulder peak on the ZnO chromatogram between 3.5 and 4 of $\log(M_w)$ was observed and the size of the shoulder peak was larger than that of the blank test. This suggests that the ZnO catalyst had a negative effect on the depolymerization of alginate in subcritical water. On the other hand, the CaO catalyst accelerated the alginate degradation and produced relatively large amounts of molecules smaller than monomers, compared to the other two reactions.

3.3.5 Reaction pathway

The reaction pathway for the hydrothermal conversion of alginate over solid base catalysts has not been studied over the past few decades. Whistler et al. suggested a reaction pathway for the formation of 3-deoxy-2-C-hydroxymethylpentaric acid from alginates by isomerization and dehydration at temperatures from 80 to 120 °C [78], however, other organic acids produced by the hydrothermal decomposition of alginate were not analyzed. Niemela et al. suggested reaction pathways for alkaline decomposition of galacturonic acid,

an isomer of alginate monomers, into various organic acids at 80 °C for 3 h [61]. They proposed that lactic acid was produced from pyruvaldehyde via benzilic acid rearrangement catalyzed by Brønsted base. The intermediates in the production of lactic acid from galacturonic acid were dihydroxyacetone, glyceraldehyde and pyruvaldehyde. These are identical to the intermediates produced by hydrothermal decomposition of glucose with base catalysts [52, 76, 88], suggesting that the same reactions, such as retro-aldol condensation, dehydration, isomerization and benzilic acid rearrangement, take place in hydrothermal reactions of both galacturonic acid and glucose.

Based on previous studies in Chapter 2 and current results, plausible reaction pathways for the hydrothermal conversion of sodium alginate into lactic acid and α-hydroxyglutaric acid with the CaO catalyst were proposed as shown in Figure 3-15-(a) and Figure 3-15-(b), respectively. As evidence of the proposed reaction pathways, the intermediates generated in the reaction was identified using LC-MS, as shown in Figure 3-15-(c). The production of lactic acid is triggered by the isomerization of sodium alginate monomers to hex-5-ulosonate, followed by the dissociation of hex-5-ulosonate into 2-hydroxy-3-oxopropanate and dihydroxyacetone via retro-aldol condensation. Dihydroxyacetone is isomerized to glyceraldehyde and pyruvaldehyde is produced by the β-hydroxy elimination of glyceraldehyde. However, these intermediates were not observed in the hydrothermal decomposition of alginate over the CaO catalyst, indicating that the conversion of the intermediates to lactic acid was promoted by the addition of the CaO catalyst. For example, pyruvaldehyde, a precursor of lactic acid, was observed in the absence of catalyst at 200 °C as shown in Figure 3-16-(a), whereas there was no pyruvaldehyde in the hydrothermal reaction over the CaO catalyst as shown in

Figure 3-16-(b). This result suggests that the conversion of pyruvaldehyde to lactic acid is the rate-determining step. In this regard, it can be proposed that the CaO catalyst enhances the conversion of pyruvaldehyde to lactic acid via a catalyst-aided benzilic acid rearrangement as described in Figure 3-15-(a). As the first step, the dissociative adsorption of water molecules occurs on the Ca^{2+}-O^{2-} pair sites, producing Brønsted base (OH^-). The OH^- attacks the carbon in carbonyl group and the attacked intermediate adsorbs onto CaO via an interaction with the Lewis acid site. In the resulting catalyst and intermediate complex, a hydrogen shift occurs and the intermediate desorbs from the catalyst surface, transforming into a lactate ion, which becomes lactic acid after the protonation of lactate. On the other hand, when dehydration occurs at C-3 of the alginate monomers instead of isomerization, the final product is α-hydroxyglutaric acid as shown in Figure 3-15-(b). After the dehydration, the loss of formate occurs and dehydration occurs again at C-3, producing 4-formyl-4-oxobutanoic acid[49], a precursor of α-hydroxyglutaric acid. Analogous to the conversion of glyceraldehyde to lactic acid, this carbonyl compound is transformed to α-hydroxyglutaric acid through the catalyst-aided benzilic acid rearrangement. The rate-determining step in this reaction cannot be suggested because the intermediates could not be prepared using standard chemicals. As shown in Figure 3-15-(c), the peak intensities for the precursors of lactic acid and α-hydroxyglutaric acid are considerably low in the ESI-MS spectrum. This might be explained by fact that the catalytic conversions of precursor compounds into lactic acid or α-hydroxyglutaric acid are significantly faster in the reaction conditions. In summary, the abundant Brønsted base from the CaO catalyst are believed to catalyze the production of lactic acid and α-hydroxyglutaric acid via the two different reaction pathways.

Table 3-1. Comparison of surface area, density of basic sites and organic acid yields from alginate over various catalysts.

Catalyst	Surface area ($m^2 g^{-1}$)	CO_2 desorbed (mmol m^{-2})			Yields of organic acids (mol%)[b]				
		Weak (T<300 °C)	Medium (300<T<500 °C)	Strong (T>500 °C)	LA	HGA	GA	AA	FA
Blank	-	-	-	-	0.74	0.88	1.36	2.30	6.67
Al_2O_3	241	6.43×10^{-4}	-	4.77×10^{-4}	0.69	1.84	1.37	2.24	7.06
Mg_{30}/Al_{70}	169	1.04×10^{-3}	1.20×10^{-3}	-	1.63	3.52	1.13	0.60	8.60
Hydrotalcite	169	1.18×10^{-3}	1.09×10^{-3}	8.35×10^{-5}	4.85	3.41	1.18	0.17	8.46
MgO	86	5.61×10^{-3}	-	7.85×10^{-4}	3.36	5.26	0.90	0.72	7.71
CaO	8.7	2.66×10^{-3}	1.61×10^{-2}	4.02×10^{-2}	12.66	3.84	0.97	0.34	7.60
ZnO	4.6	2.15×10^{-3}	5.39×10^{-3}	-	0.68	1.05	1.71	1.06	7.75
ZrO_2	23	4.80×10^{-3}	1.78×10^{-3}	-	0.83	0.60	1.60	1.79	7.86
CeO_2	126	1.35×10^{-3}	8.91×10^{-4}	-	1.98	2.09	1.53	1.55	7.89
TiO_2	9.9	1.81×10^{-3}	-	-	0.79	1.47	2.51	1.30	8.08

* Sodium alginate=600 mg, catalyst=600 mg, solvent (water)=30 mL, reaction temperature=200 °C, reaction time=1 h, stirring speed=600 rpm.

* LA: lactic acid, HGA: α-hydroxyglutaric acid, GA: glycolic acid, AA: acetic acid, FA: formic acid.

Table 3-2. Effect of reactant (sodium alginate) on the reusability test with the CaO catalyst.

Reaction	Addition of reactant	Yields of organic acids (mol%)[b]				
		LA	HGA	GA	AA	FA
1st	Yes	12.59	4.44	0.35	1.08	7.59
2nd	No	1.67	1.00	0.14	0.30	0.55
3rd	Yes	11.95	3.95	0.62	0.74	7.87
4th	No	1.68	1.95	0.13	0.60	0.57
5th	Yes	2.66	3.88	0.64	0.65	10.22

* Sodium alginate=600 mg, catalyst=600 mg, solvent (water)=30 mL, reaction temperature=200 °C, reaction time=1 h, stirring speed=600 rpm.

* LA: lactic acid, HGA: α-hydroxyglutaric acid, GA: glycolic acid, AA: acetic acid, FA: formic acid.

Table 3-3. Molecular distribution of raw alginate and hydrothermally treated alginate over different metal oxide catalysts.

Sample	M_w (Da)	M_n (Da)	PDI
Raw alginate	277865	65185	4.26
Blank	1934	1216	1.59
Al_2O_3	1684	959	1.76
Mg_{30}/Al_{70}	1607	973	1.65
Hydrotalcite	1666	1200	1.39
MgO	1881	1313	1.43
CaO	1582	1128	1.40
ZnO	2207	1286	1.72
ZrO_2	1839	1012	1.82
CeO_2	1487	1014	1.47
TiO_2	1648	959	1.72

* Sodium alginate: 600 mg, catalyst: 600 mg, solvent (water): 30 mL, reaction temperature: 200 °C, reaction time: 1 h, stirring speed: 600 rpm.

* Weight average molecular weight (M_w).

* Number average molecular weight (M_n).

* Polydispersity index (PDI) = M_w/M_n.

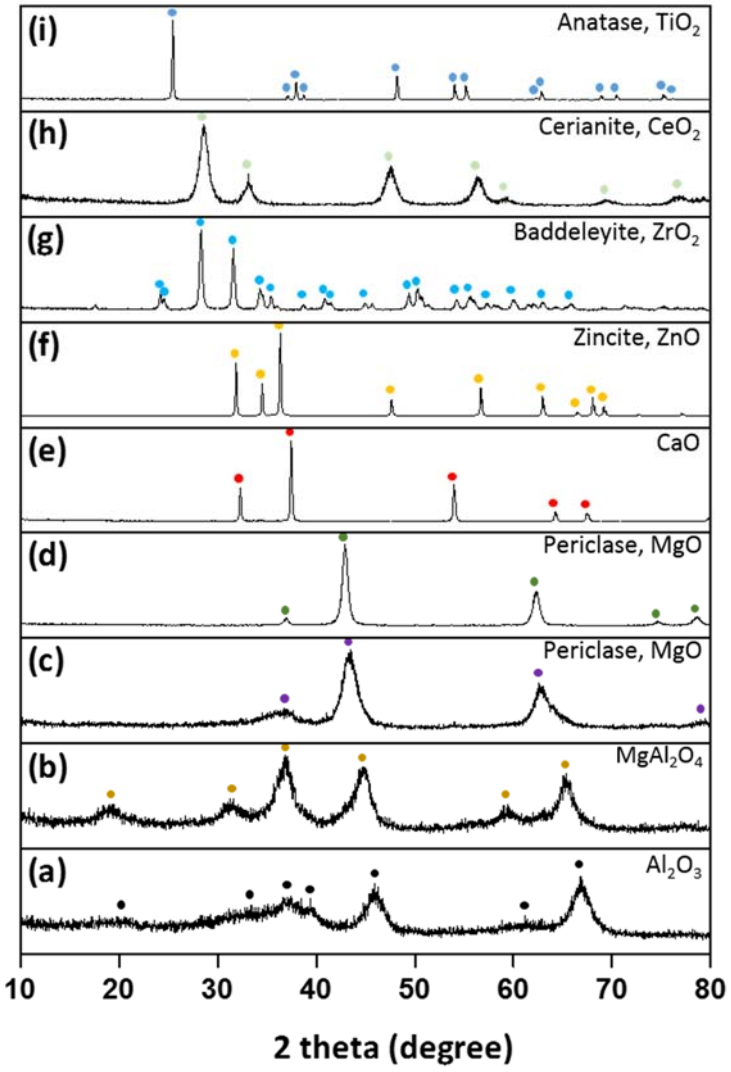

Figure 3-1. X-ray diffraction patterns of prepared solid base catalysts: (a) Al_2O_3, (b) $Mg_{30}Al_{70}$, (c) hydrotalcite, (d) MgO, (e) CaO, (f) ZnO, (g) ZrO_2, (h) CeO_2, (i) TiO_2.

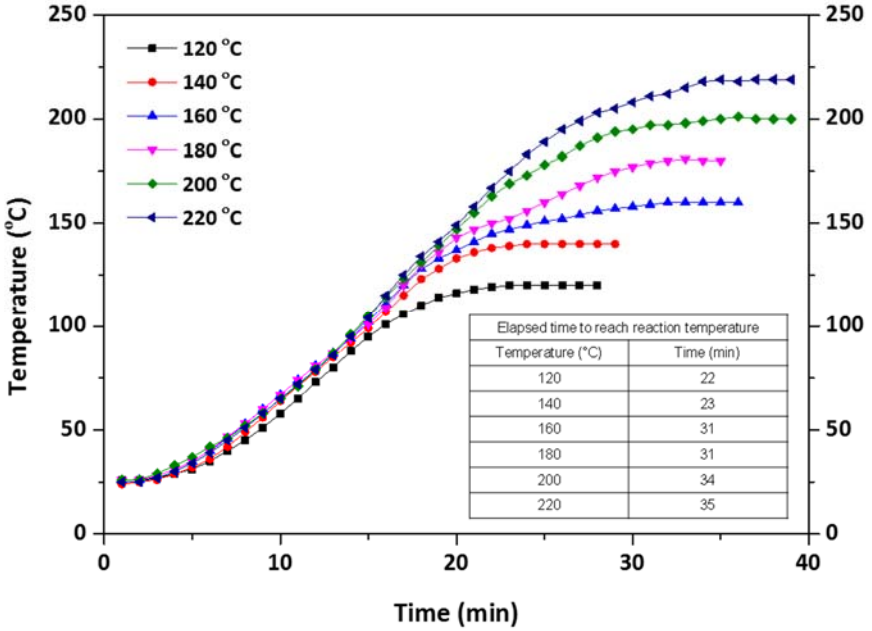

Figure 3-2. Temperature profile of a reactor for different target temperatures. Reactor volume= 50 mL, water= 30 mL, stirring speed= 600 rpm.

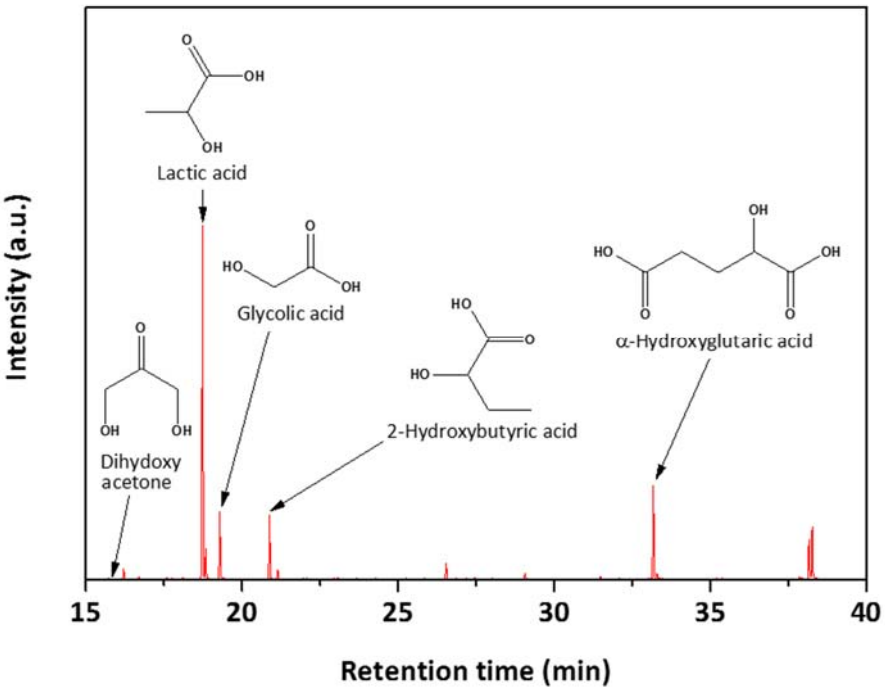

Figure 3-3. GC-MS chromatogram of a sample produced by hydrothermal conversion of alginate over CaO catalyst at 200 °C for 30 min.

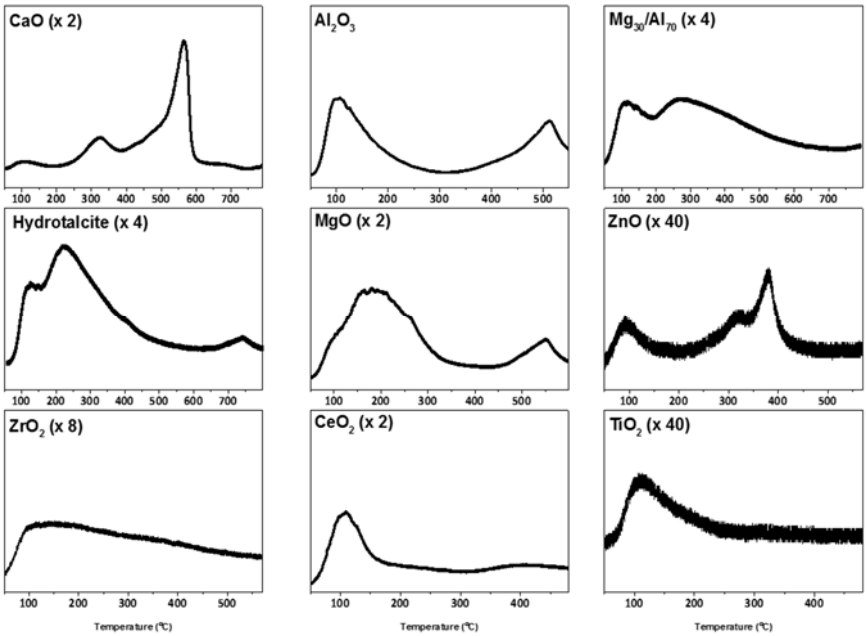

Figure 3-4. CO_2-TPD patterns of metal oxides.

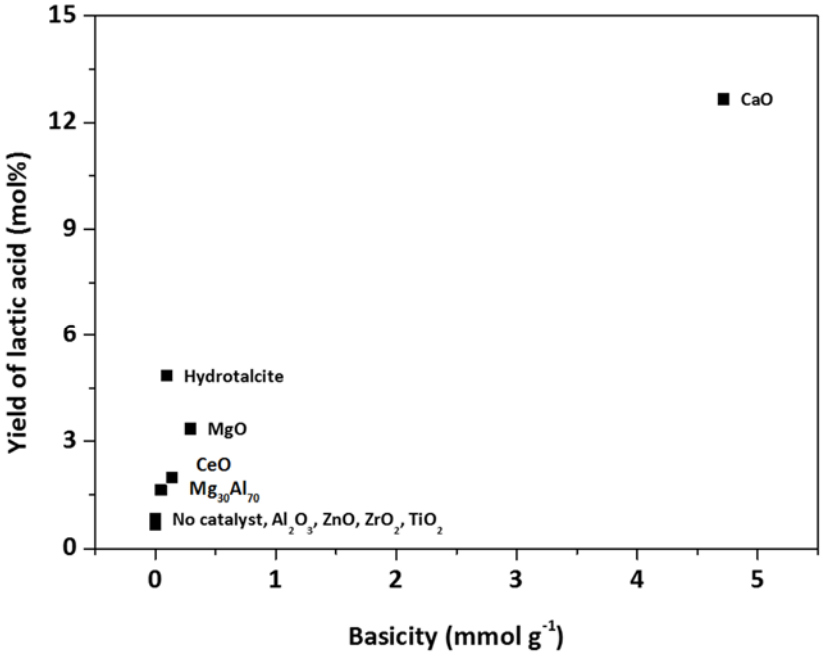

Figure 3-5. Effect of the basicity of different metal oxide catalysts in an aqueous medium on lactic acid yields. Reaction conditions: sodium alginate=600 mg, catalyst=600 mg, solvent (water)=30 mL, reaction temperature=200 °C, reaction time=1 h, stirring speed=600 rpm.

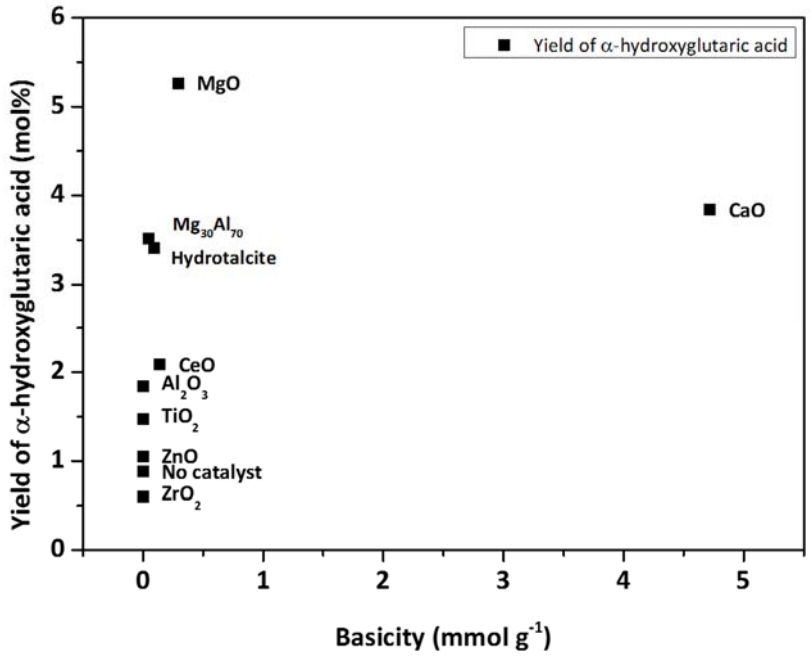

Figure 3-6. Effect of basicity of different metal oxide catalysts on yields of α-hydroxyglutaric acid. Yields of α-hydroxyglutaric acid (orange column). Amount of basicity (■). Reaction conditions: sodium alginate=600 mg, catalyst=600 mg, solvent (water)=30 mL, reaction temperature=200 °C, reaction time=1 h, stirring speed=600 rpm.

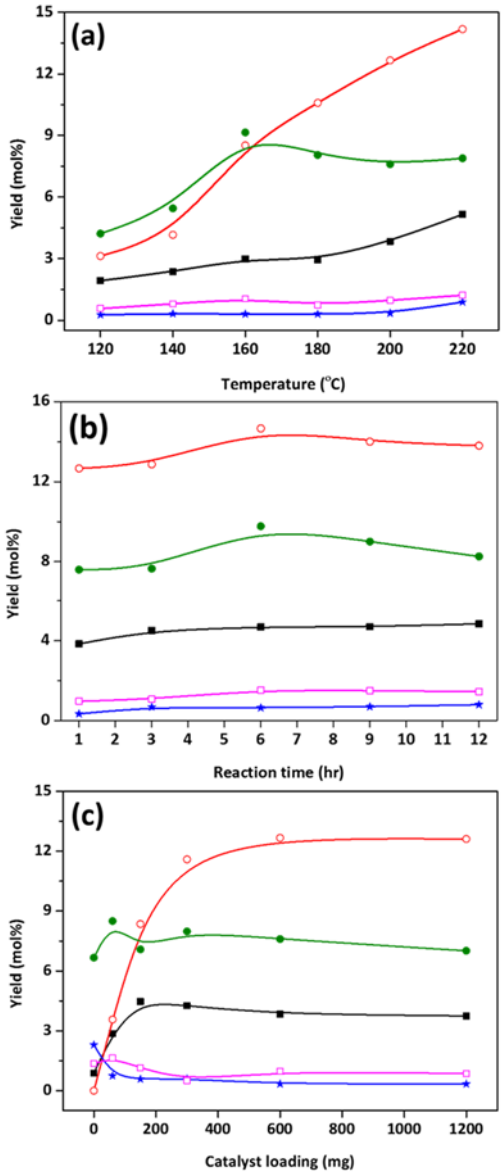

Figure 3-7. Yields of organic acids produced by hydrothermal treatment of alginate over CaO catalyst in different reaction conditions; (a) reaction temperature, (b) reaction time, (c) catalyst loading. α-Hydroxyglutaric acid (■). Lactic acid (○). Glycolic acid (★). Acetic acid (□). Formic acid (●). Reaction conditions: sodium alginate=600 mg, catalyst=600 mg, solvent (water)=30 mL, reaction temperature=200 °C, stirring speed=600 rpm.

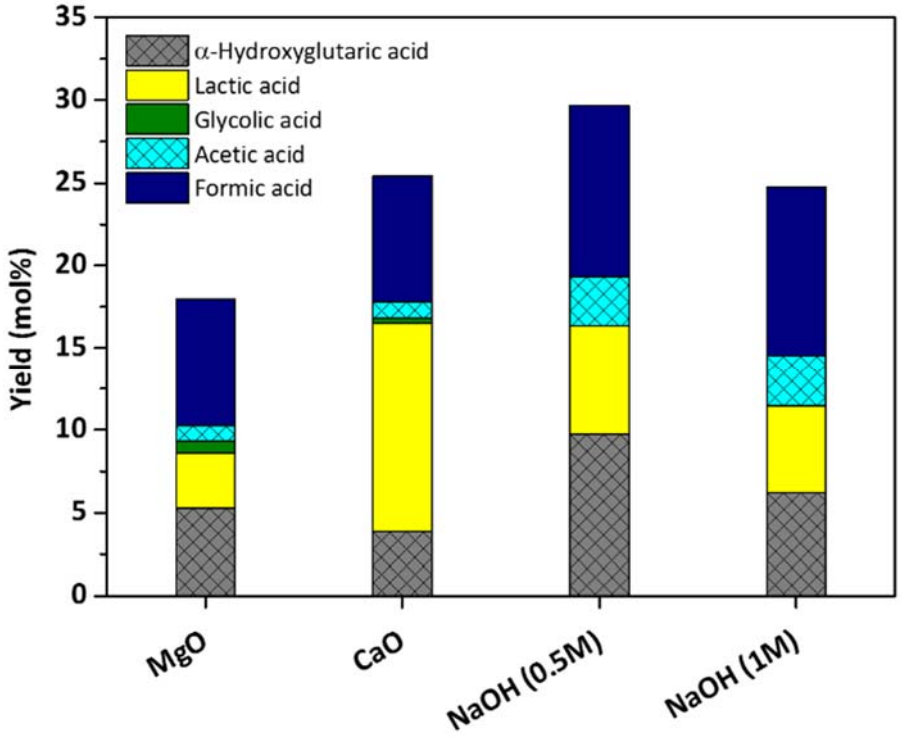

Figure 3-8. Comparison of yields of organic acids produced via hydrothermal conversion of sodium alginate over heterogeneous and homogeneous catalysts. Reaction conditions: sodium alginate=600 mg, metal oxide catalyst=600 mg, solvent (water or NaOH solution)=30 mL, reaction temperature=200 °C, reaction time=1 h, stirring speed=600 rpm.

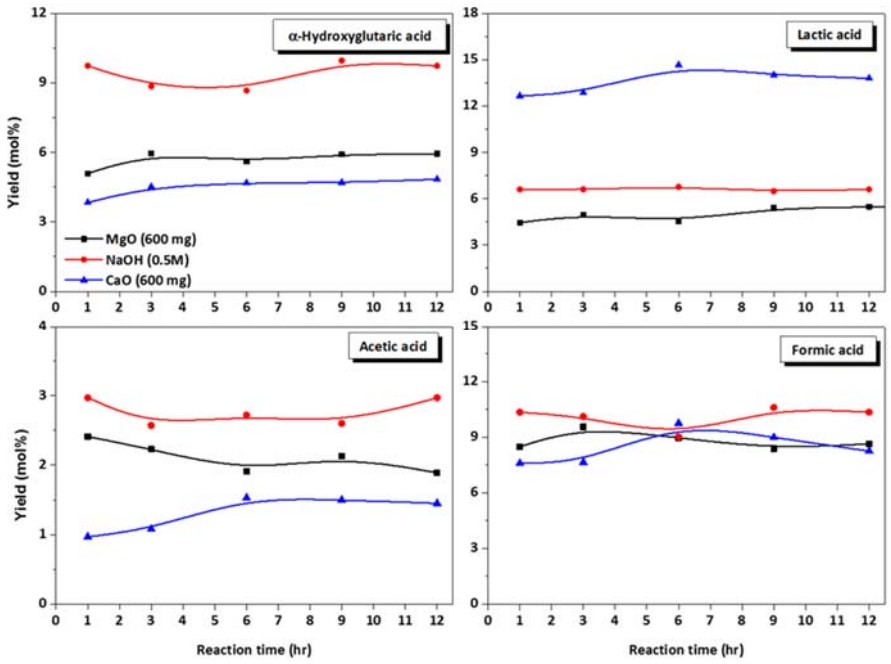

Figure 3-9. Comparison of catalytic activity between heterogeneous and homogeneous base catalysts by reaction times. Reaction conditions: sodium alginate=600 mg, solvent (water)=30 mL, reaction temperature=200 °C, stirring speed=600 rpm.

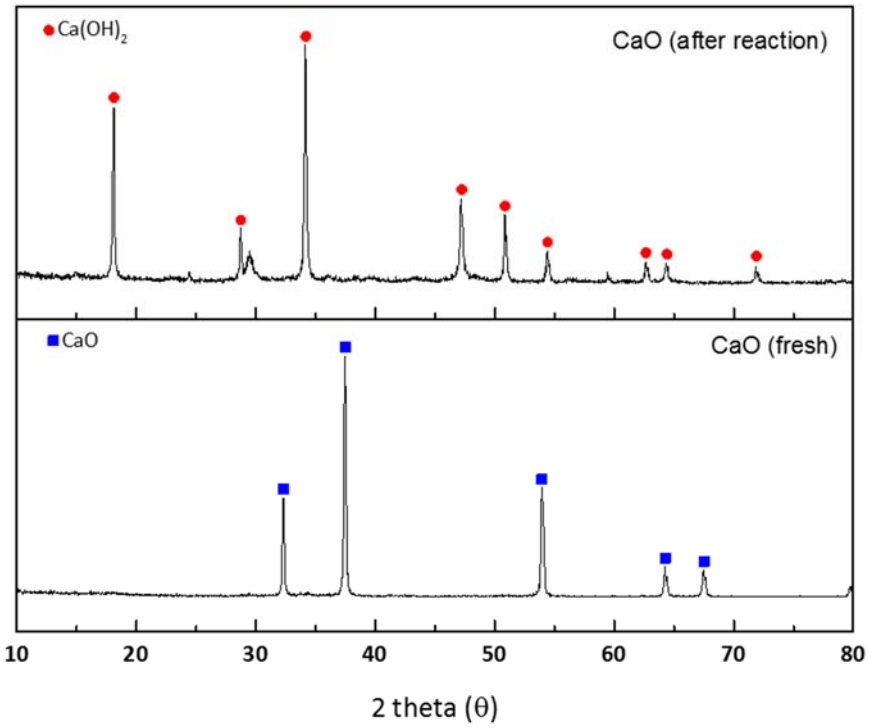

Figure 3-10. XRD patterns of fresh and used CaO catalysts. Reaction conditions: sodium alginate=600 mg, catalyst=600 mg, solvent (water)=30 mL, reaction temperature=200 °C, reaction time=1 h, stirring speed=600 rpm.

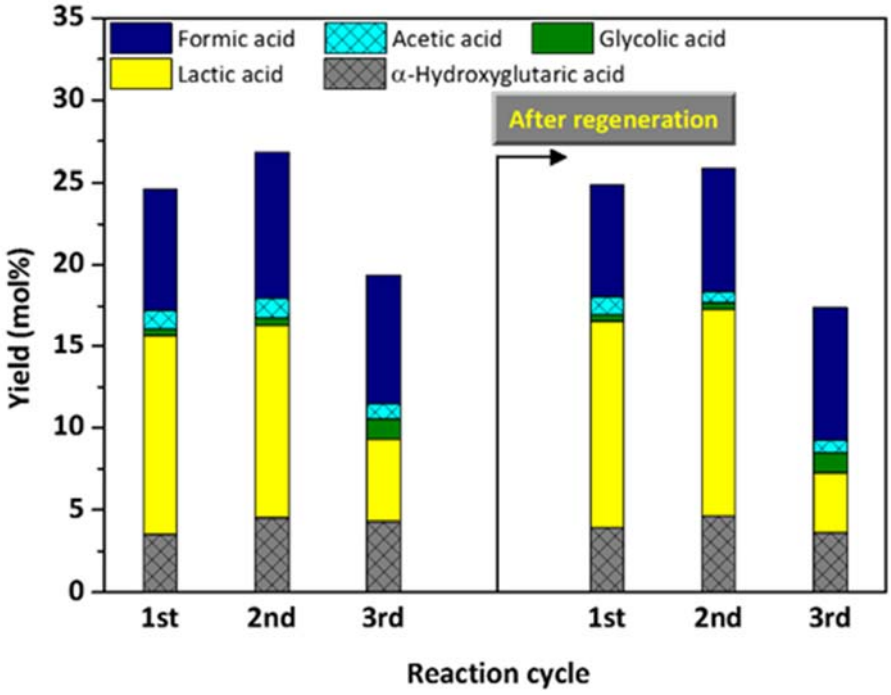

Figure 3-11. Effect of reuse and regeneration of CaO catalyst on the yields of organic acids by the hydrothermal conversion of alginate. Reaction conditions: sodium alginate=600 mg, catalyst=600 mg, solvent (water)=30 mL, reaction temperature=200 °C, reaction time=1 h, stirring speed=600 rpm. Regeneration conditions: 800 °C for 5 h in ambient atmosphere.

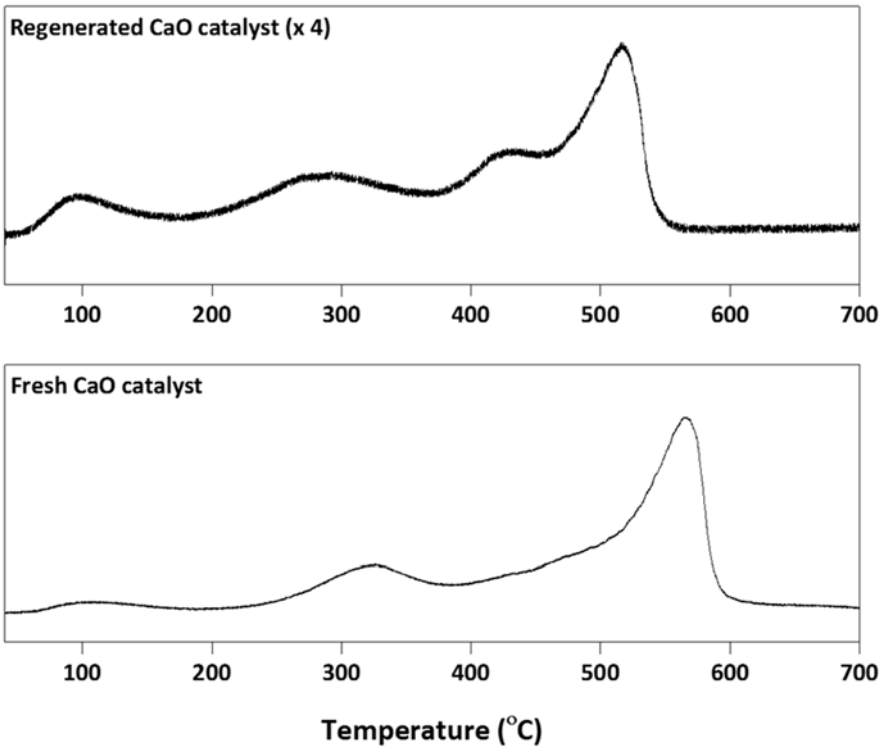

Figure 3-12. CO_2-TPD patterns of fresh and regenerated CaO catalysts. Regeneration condition: 800 °C for 5 h.

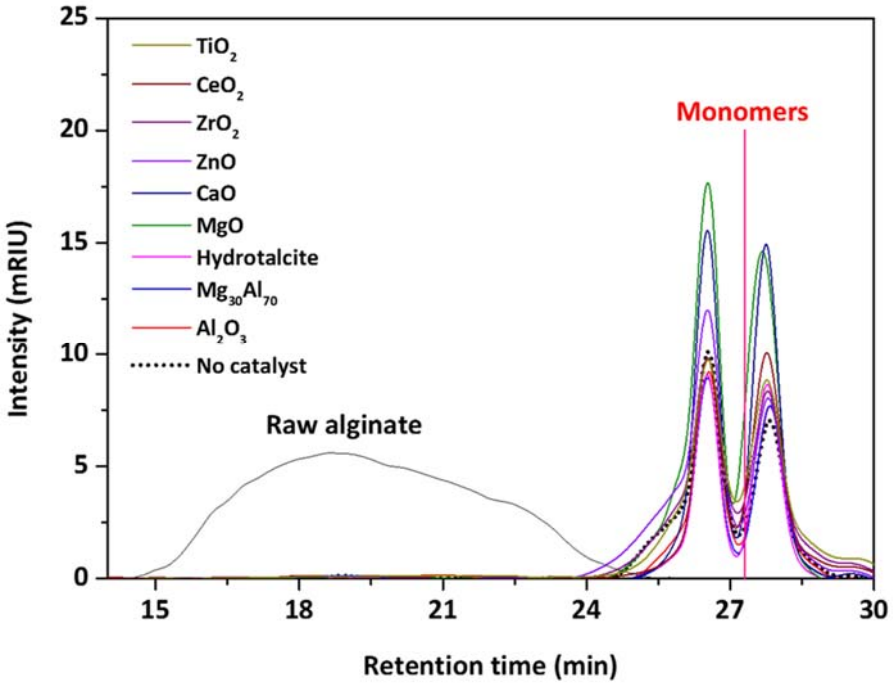

Figure 3-13. GPC chromatograms of raw alginate and hydrothermally treated alginate over various metal oxide catalysts at 200 °C for 1 h.

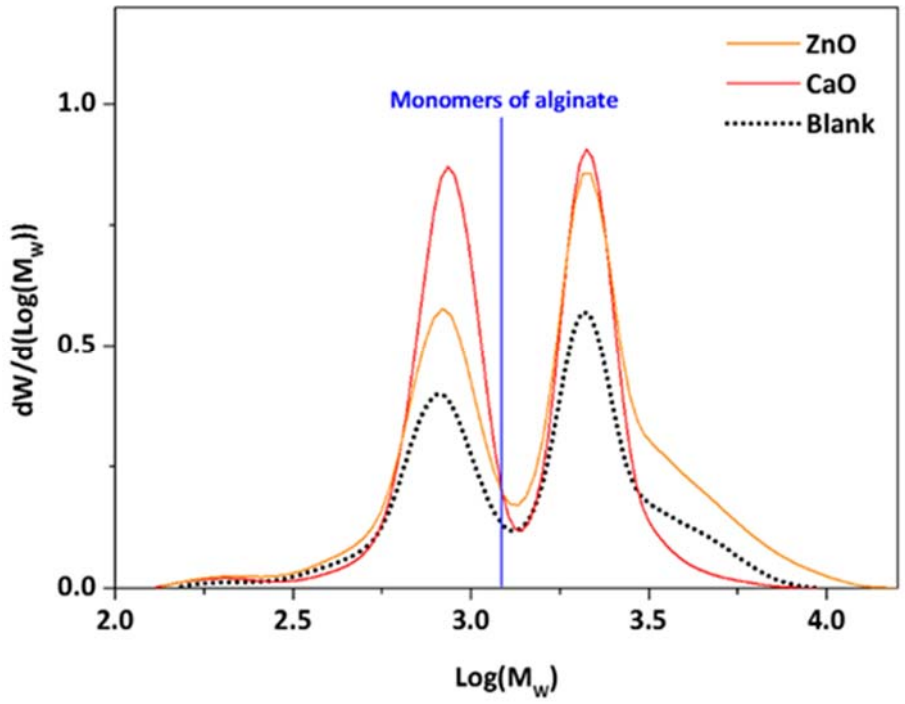

Figure 3-14. Comparison of molecular distribution curves obtained by hydrothermal treatment of alginate over CaO and ZnO at 200 °C for 1 h. M_w is the weight average molecular weight. dW/d(Log(M_w)) is the weight fraction of molecules at M_w. Blank reaction (black dot line). CaO (red solid line). ZnO (orange solid line).

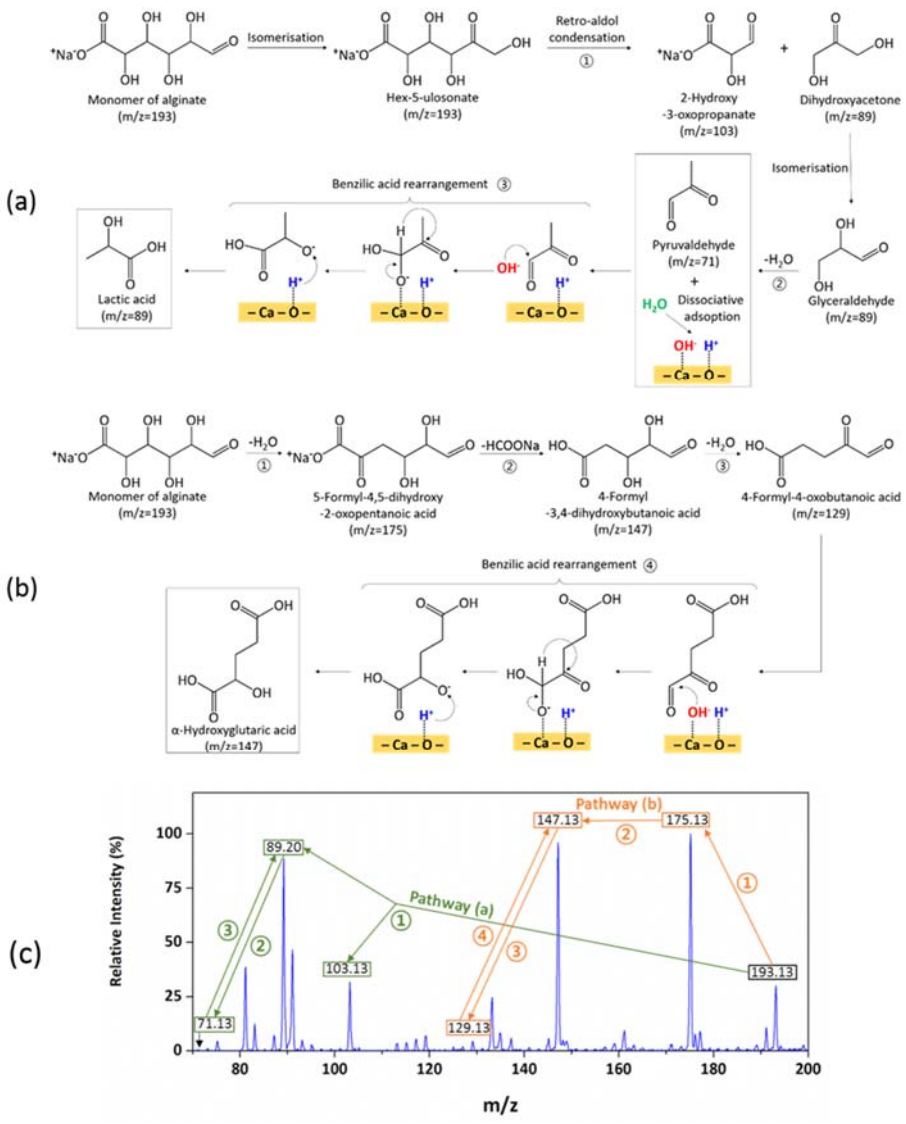

Figure 3-15. Proposed reaction pathways for catalytic hydrothermal conversion of sodium alginate into lactic acid and α-hydroxyglutaric acid under CaO catalyst. (a) Reaction pathway for production of lactic acid; (b) Reaction pathway for production of α-hydroxyglutaric acid; (c) ESI-MS spectrum obtained at a negative mode for hydrothermally treated alginate over CaO catalyst at 200 °C for 1 h.

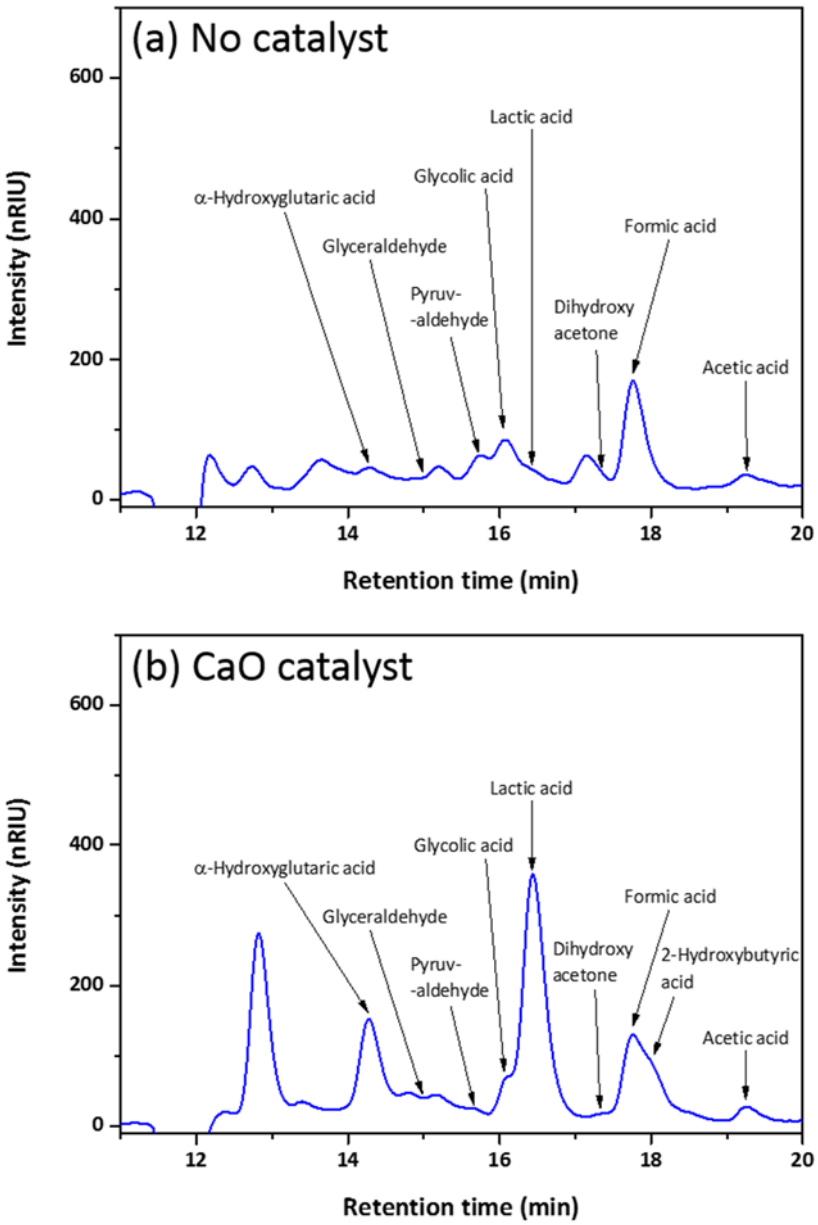

Figure 3-16. HPLC-RID chromatogram for hydrothermal decomposition of alginate at 200 °C for 1 h. (a) Reaction without catalyst; (b) Reaction over CaO catalyst (600 mg).

Chapter 4. Production of Furfural from Alginic Acid Catalyzed by Metal Cations in Hydrothermal Conditions

4.1 Introduction

Alginic acid, composed of two kinds of hexuronic acids such as β-D-mannuronic acid and α-L-guluronic acid, is one of major carbohydrate compounds contained in macroalgae like brown seaweeds [89]. Recently, this biopolymer is extensively used in biochemical processes in order to produce high value-added chemicals like bioethanol or volatile fatty acids (VFAs) [90-93]. Unlike cellulose, alginate is composed of monomers containing a carboxyl group, ascribed to the production of organic acids in hydrothermal decomposition of alginate. Niemela and Sjostrom [49] used NaOH and $Ca(OH)_2$ as a base catalyst for the hydrothermal decomposition of alginate. As a result, numerous di- and mono-carboxylic acids were produced at relatively low reaction temperatures, 95 and 135 °C. Main products in the base-catalyzed hydrothermal reaction were lactic acid, α-hydroxyglutaric acid and glucoisosaccharinaric acid. In the absence of catalysts, the hot-compressed water can act as acid and base catalysts itself [26]. Aida et al. [51] treated alginate in sub- and super-critical water with a view to producing organic acids. In their study, main products were formic acid and malic acid at 150 °C, however, lactic acid was produced by the base-catalyzed reaction at 350 and 450 °C without adding any base catalysts. In previous study presented in Chapter 2, the effect of pH on the product distribution of organic acids was studied with using HCl and NaOH as Arrhenius acid and base catalysts,

respectively [79]. It was found that acid-catalyzed hydrothermal treatment of alginate yielded the furan compounds, such as furfural and 2-furoic acid, in addition to various organic acids. In particular, the yield of furfural was approximately 10 % at 200 °C and pH 1 within 60 min, exhibiting the possibility that furfural can be synthesized by the hydrothermal conversion of alginic acid instead of hemicellulose.

Furfural is an important platform chemical for sustainable production of fuels and other valuable chemicals. This renewable and non-petroleum-derived chemical can be utilized in a wide range of applications, such as plastics, agrochemicals, pharmaceuticals, fragrances and fuel additives [94, 95]. In spite of the wide spectrum of applications, it is known that there is no synthetic route available to produce furfural except the conversion of lignocellulosic biomass [96]. A representative process for the furfural production from lignocellulosic biomass is the acid-catalyzed hydrolysis and dehydration of hemicellulose [97-99]. Unlike cellulose and lignin, hemicellulose is mainly composed of C5 sugars like xylose or arabinose. This structure of hemicellulose is favorable for the selective production of furfural, since pentose tends to convert to furfural over acid catalysts in aqueous reaction medium. For example, Choudhary et al. [100] reported that the yield of furfural was 23.5 % when xylose was reacted at 110 °C for 60 min over Amberlyst-15, as a solid acid catalyst, in an aqueous medium. Sahu and Dhepe [101] studied the effect of biphasic reaction system on the hydrothermal conversion of hemicellulose to furfural using solid acid catalysts. The addition of organic solvents into the aqueous medium in order to establish the biphasic reaction system significantly enhanced the production of furfural while inhibiting the degradation of furfural. So far, the catalytic hydrothermal production of furfural from hemicellulose or xylose has been

extensively studied for high furfural yields [102, 103].

Herein, the effect of metal cations on the hydrothermal conversion of alginic acid to furfural was investigated. As catalysts, various metal cations were used to investigate the effect of metal cations on the hydrothermal decomposition of alginate. The effect of experimental conditions, such as temperature, time and catalyst concentration, was also studied. In this experiment, alginic acid, not a salt form, was used as a reactant in order to analyze the function of metal cations in the hydrothermal reaction, since different kinds of metal ions like Na^+, Ca^{2+} and K^+ contained in alginic acid salts may interfere in the hydrothermal reaction.

4.2 Experimental

4.2.1. Preparation of metal ion solutions

The metal cation solutions were prepared with various metal nitrate compounds. The metal nitrate compounds used in this research are the following: $Cr(NO_3)_3 \cdot 9H_2O$ (99%), $Mn(NO_3)_2 \cdot 4H_2O$ (>97%), $Fe(NO_3)_3 \cdot 9H_2O$ (>98%), $Co(NO_3)_2 \cdot 6H_2O$ (>98%), $Ni(NO_3)_2 \cdot 6H_2O$ (98%), $Cu(NO_3)_2 \cdot 3H_2O$ (99–104%), $Zn(NO_3)_2 \cdot 6H_2O$ (99%), $Y(NO_3)_3 \cdot 6H_2O$ (99.9%), $ZrO(NO_3)_2 \cdot xH_2O$ (99%), $La(NO_3)_3 \cdot 6H_2O$ (99.99%), $Ce(NO_3)_3 \cdot 6H_2O$ (99%), $Pr(NO_3)_3 \cdot 6H_2O$ (99.9%), $Nd(NO_3)_3 \cdot 6H_2O$ (99.9%), $Gd(NO_3)_3 \cdot 6H_2O$ (99.9%), $Pb(NO_3)_2$ (>99%), $Al(NO_3)_3 \cdot 9H_2O$ (98–102%), $Ga(NO)_3 \cdot xH_2O$ (99.9%). The nitrates were added into distilled water at the target concentrations, followed by stirring for 3 h at room temperature. Alginic acid obtained from brown algae was purchased from Sigma-Aldrich. This product was composed of mannuronic acid (61%) and guluronic acid (39%) approximately.

4.2.2. Reaction procedure

A Teflon-lined stainless steel batch reactor (50 mL) was used for hydrothermal treatment of alginic acid. A stirrer was located inside the reactor for an effective contact between insoluble alginic acid and metal cations in water (600 rpm). Alginic acid (0.6 g) and metal cation solution (30 mL) were added to the reactor. The sealed reactor was purged with nitrogen gas and mounted in a heater. The elapsed time to reach a target temperature (160, 180, 200 and 220 °C) is presented in Figure 4-1. The ramping period was excluded in defining reaction

time. After dwelling at the target temperatures, the reactor was immediately quenched with a cold-water. Prior to product analysis, a liquid part was separated from solid-liquid mixture by centrifugation, followed by dilution.

4.2.3. Product analysis

Furfural and organic acids were quantified with an Agilent 1200 Series HPLC equipped with two Shodex RSpak KC-811 columns in series. RI detector (Agilent G1362A) and UV detector (Agilent G1314B) were used together for crosschecking the data. The wavelength of the UV detector was set to 210 nm in order to observe furfural and organic acids simultaneously. Phosphoric acid aqueous solution (5 mM), as a mobile phase, was run through the column (40 °C) at a flow rate of 1.0 mL min^{-1}.

The molecular weight distribution of products was analyzed by gel permeation chromatography (GPC). The GPC system (Ultimate 3000, Dionex) was composed of three types of columns (Waters Ultrahydrogel column: 120, 500 and 1000) in series. Sodium azide solution (0.1 M), as a mobile phase, flowed through the colum (40 °C) at a flow rate of 1.0 mL min^{-1}. Pullulan with a molecular weight distribution from 342 to 80500 was used to calibrate the GPC system.

Furfural and intermediates of the hydrothermal reaction were identified with a LC-MS system (Surveyor, Thermo Finnigan) in combination with a mass spectrometer (LCQ Deca XP Plus, Thermo Finnigan) equipped with an electrospray ionization module and working in positive or negative mode with a capillary temperature of 275 °C. Three types of mobile phases (0.1% of formic acid dissolved in distilled water, acetonitrile or methanol) were run through a

column (Synergi™ 4 µm Polar-RP 80 Å, LC Column 150 x 2 mm, Phenomenex) at a flow rate of 0.25 mL min^{-1}. The UV wavelength was set from 210 to 280 nm.

4.3 Results and discussion

4.3.1 Effect of metal cations on conversion of alginic acid to furfural

The hydrothermal treatment of alginic acid to furfural was executed at 200 °C for 30 min, with various metal cations as a catalyst. As shown in Figure 4-2, Cu (II) ions shows the highest furfural yield (13.19 %) higher than two times the furfural yield obtained in a blank test (5.14 %). Based on the furfural yield of the blank test, Cu (II), Fe (III) and Pb (II) ions promoted the conversion of alginic acid to furfural. In the hydrothermal reaction under Zn (II), Co (II) and Ni (II) ions, there was little or no catalytic effect. Other metal cations except the six metal cations mentioned above inhibited the production of furfural rather than catalyzing it. In particular, the yield of furfural decreased from 5.14 % to 2.5 % when Y (III) ions participated in the reaction. Generally, xylose obtained by hydrolysis of hemicellulose is sequentially dehydrated to furfural in the hydrothermal conversion of hemicellulose [104, 105]. In contrast, glucose, a monomer of cellulose, tends to convert to hydroxymethylfufrual (HMF) rather than furfural, since glucose has an extra alcohol functional group compared to xylose [106]. The conversion of HMF to furfural was feasible via the loss of formaldehyde in HMF, but it is not favorable [107]. In the same manner, the carboxylic functional group of mannuronic acid and guluronic acid should be eliminated to produce furfural from alginic acid. In other words, both decarboxylation and dehydration are important reaction steps for the conversion of alginic acid to furfural, and those reaction steps are significantly dependent on the kind of metal cations

The physical or chemical properties of the metal ions were correlated with the

yields of furfural, in order to explain the effect of metal cations on the production of furfural from alginic acid. Figure 4-3 shows the correlation between the furfural yield and ionic radius of metal ions. For lanthanide metal ions, the yield of furfural linearly increases with the ionic radius of the metal ions. However, the lanthanide metal cations shows poor catalytic performance in the production of furfural, showing lower furfural yields than that of the blank test. The yields of furfural for post-transition metal ions are also proportional to the size of metal ions. The largest metal ions, Pb (II) (119 pm), exhibits the highest furfural yield (7.12 %) among the post-transition metal ions. On the other hand, there was no clear relation between the furfural yield and the ionic radius of transition metal cations. The transition metal ions show better catalytic performance than other two groups of metal ions for the production of furfural from alginic acid.

As shown in Figure 4-4, the yields of furfural are almost proportional to the electronegativity in Pauling scale. The strong electronegativity of metal cations suggests that the metal ions can play a role of Lewis acid catalysts in the hydrothermal conversion of alginic acid, since the electronegative metal ions attract electrons towards itself, promoting the electron transfer in the reaction. Lewis acidity is proportional to the electronegativity of metal cations [108], which may lead to the acid-catalyzed dehydration in the conversion of alginic acid to furfural. On the contrary, the furfural yields under the lanthanide metal ions are reversely proportional to the electronegativity of the metal ions, suggesting that the lanthanide metal ions can participate in the hydrothermal reaction of alginic acid via a different reaction path.

From the hydrothermal reaction of alginic acid, a few organic acids were also produced with furfural. As listed in Table 4-1, glycolic acid, lactic acid and

formic acid were mainly produced with furfural in the conversion of alginic acid at 200 °C for 30 min. In the blank test, 0.32 % of glycolic acid and 2.36 % of formic acid were formed with 5.14 % of furfural. The Cu (II) ions yielded relatively small amounts of organic acids compared to other metal cations, while the Cu (II) ions exhibited the best catalytic performance in the production of furfural. This indicates that Cu (II) ions can convert alginic acid to furfural more selectively than different metal ions. The highest yield of glycolic acid was achieved in the reaction under Cr (III) ions. The production of both furfural and glycolic acid is an evidence of which the acid-catalyzed reaction took place in the conversion of alginic acid due to Brønsted acid (H^+) provided from alginic acid in the aqueous reaction medium [79]. However, relatively high amounts of lactic acid were produced under Pb (II), Ga (III) and Al (III) ions, implying that the post-transition metal cations likely promoted both the acid- and base-catalyzed hydrothermal reactions of alginic acid.

By the way, the yield of formic acid is reversely proportional to that of furfural as shown in Figure 4-5. In previous research introduced in Chapter 2, it was observed that furfural mainly concerted to formic acid and water-insoluble humins in hydrothermal conditions [79]. Therefore, the high yield of formic acid with the low yield of furfural can be explained by the decomposition of furfural under metal cations, such as Gd (III) and Y (III) ions. However, Cu (II) and Fe (III) ions seem to make furfural produced stable in the acidic hydrothermal condition. Otherwise, more formic acid should be produced by the decomposition of furfural under Cu (II) and Fe (III) ions, because these two metal ions yield the larger amount of furfural, compared to other metal cations.

4.3.2 Influence of reaction conditions on production of furfural

The hydrothermal treatments of alginic acid at different reaction temperatures and times were performed to study the effect of reaction conditions on the production of furfural. As shown in Figure 4-6, the reaction temperature and time strongly influenced the production of furfural. When Cu (II) ions were used as a catalyst, the yield of furfural significantly increased compared to the blank test at 200 °C. The maximum furfural yield (13.19 %) was obtained at 200 °C in 30 min, however, it rapidly decreased to 5.34 % for next 30 min. The decreasing furfural yield after 30 min seems to be ascribed to the hydrothermal conversion of furfural to formic acid or humin compounds. At 220 °C, the maximum value of furfural yield could not be observed, which can be explained as furfural produced began to be degraded or polymerized prior to reaching to the target temperature due to a sufficiently long ramping period, approximately 30min. At lower temperatures than 200 °C, both the maximum furfural yields and the production rates of furfural were lower than at 200 °C. For instance, the yield of furfural reached to the maximum value, 9.53 %, at 160 °C after 180 min and it was constant after next 180 min, indicating that furfural is hydrothermally stable at 160 °C.

The concentration of metal ions also strongly influenced the yield of furfural, as plotted in Figure 4-7. Interestingly, there was an optimal concentration of Cu (II) ions for the highest furfural yield. When the hydrothermal treatment of alginic acid was conducted at 200 °C under 0.01 M of Cu (II) ions, 13.19 % of furfural was produced. As the Cu (II) concentration increased from 0.0025 M to 0.01 M, the yield of furfural rose from 7.39 % to 13.19 %, which means that the increasing Cu (II) ions further catalyzed the conversion of alginic acid to furfural as Lewis acid catalysts. On the other hand, higher concentrations of Cu

(II) ions than 0.01 M was likely to inhibit the conversion of alginic acid to furfural rather than catalyzing it. The excess Cu (II) ions seems to unselectively react with oxygen atoms of alginic acid, leading to side reactions. For example, the metal ions can interact with oxygen atoms of each carboxyl group of alginic acid and thus bidentate chelate compounds are formed [109], which might inhibit the decarboxylation of alginic acid monomers.

4.3.3 Effect of metal cations on hydrothermal depolymerization of alginic acid

The influence of metal ions on the depolymerization of alginic acid was visualized on GPC chromatograms in Figure 4-8. Compared to the blank test, Y (III) ions catalyzed the degradation of alginic acid, while the catalytic effect by Cu (II) ions were insignificant. As mentioned above, Cu (II) and Y (III) ions exhibited the highest and lowest furfural yield in the conversion of alginic acid, respectively. Based on the peak of monomer, Y (III) ions promoted the production of smaller molecules than monomers, mannuronic acid and guluronic acid. Y (III) ions are effective for the hydrothermal decomposition of alginic acid, but not for the production of furfural. On the contrary, Cu (II) ions are favorable for the conversion of alginic acid to furfural in spite of the relatively low catalytic performance for degrading alginic acid. The concentration of metal ions also influences the depolymerization of alginic acid as listed in Table 4-2. The sample produced in 0.01 M of Cu (II) ion solution has the highest weight average molecular weight (M_w) with the highest polydispersity index (PDI) value, indicating that the Cu (II) concentration shows relatively low catalytic performance in the depolymerization of alginic acid with a wide molecular weight distribution of liquid product, compared to

different Cu (II) concentrations. The relation between the Cu (II) concentration and the PDI value is similar with that between the Cu (II) concentration and the furfural yield as shown in Figure 4-7. This suggests that furfural is produced more abundantly when alginic acid is degraded with the wide molecular weight distribution.

4.3.4 Reaction pathway of furfural production from alginic acid

When alginic acid is added into an aqueous reaction medium, Brønsted acids (H^+) are released from carboxyl groups of the monomeric units of alginic acid. The acidic reaction medium can act as an acid catalyst in the conversion of alginic acid to furfural, via catalyzing hydrolysis and dehydration reactions. In the hydrothermal conversion of xylose to furfural, Brønsted acid significantly enhances the acid-catalyzed dehydration of xylose, a key reaction for the furfural production [110, 111]. Based on the structural differences between the monomers of alginic acid and xylose, the removal of the carboxyl group is necessary for the production of furfural from alginic acid. As shown in Figure 4-9, a plausible reaction pathway for the catalytic conversion of alginic acid to furfural involves both decarboxylation and dehydration. As an evidence, carbon dioxide generated in all reactions performed as a main gaseous product, simply checked by gas chromatography equipment. Furfural and intermediates in a product sample were also detected by LC-MS analysis, as shown in Figure 4-10. Prior to the decarboxylation, the dehydration of monomer at C-3 position is necessary, since a carbonyl group near the carboxyl group is favorable for the cleavage of the linkage between C-1 and C-2 positions. The carbonyl group can be formed by keto-enol tautomerization. Metal cations can play a role of

catalyst promoting keto-enol tautomerization in hydrothermal conditions [77, 112]. In the hydrothermal reaction of alginic acid, Cu (II) ions likely catalyze the tautomerization, leading to the formation of the carbonyl group at C-2 position. After the decarboxylation, the intermediate is transformed to a ring type of compound, followed by sequential dehydration of the ring compound to furfural. In the conversion of alginic acid to furfural, the tautomerization catalyzed by metal ions is likely a key reaction determining the yield of furfural. Based on the correlation between the electronegativity and the furfural yield, it is strongly suggested that the high electronegativity enhances the keto-enol tautomerization through the electronic interaction between electrons of an oxygen atom and the electronegative metal cations.

Table 4-1. Effect of metal cations on the production of furfural and organic acids at 200 °C for 30 min.

Catalyst (0.01 M)	Yield (mol%)			
	Furfural	Glycoic acid	Lactic acid	Formic acid
Blank	5.14	0.32	-	2.36
Zn (II)	5.77	3.19	-	2.24
Cr (III)	3.75	5.87	3.34	1.96
Mn (II)	3.44	0.88	-	3.03
Co (II)	5.64	1.85	-	2.42
Ni (II)	5.02	2.44	0.95	2.79
Cu (II)	13.19	0.99	-	1.68
Fe (III)	9.43	1.61	-	1.72
Y (III)	2.5	2.15	-	4.8
Pb (II)	7.12	2.91	2.24	2.31
Ga (III)	3.49	3.76	5.63	3.33
Al (III)	3.24	4.52	6.73	3.08
Ce (III)	3.92	2.53	-	3.73
Pr (III)	3.77	1.54	-	3.97
La (III)	4.31	1.56	1.24	3.6
Nd (III)	3.66	2.60	-	4.24
Gd (III)	2.92	2.67	-	5.37

Table 4-2. Effect of Cu (II) ion concentration on the depolymerization of alginic acid at 200 °C for 30 min.

Sample	M_w (Da)	M_n (Da)	PDI
Raw alginic acid	240000	-	-
Cu (II) – 0.0025 M	1482	658	2.25
Cu (II) – 0.005 M	1452	666	2.18
Cu (II) – 0.01 M	1711	712	2.40
Cu (II) – 0.02 M	1470	937	1.57
Cu (II) – 0.04 M	1613	1148	1.40

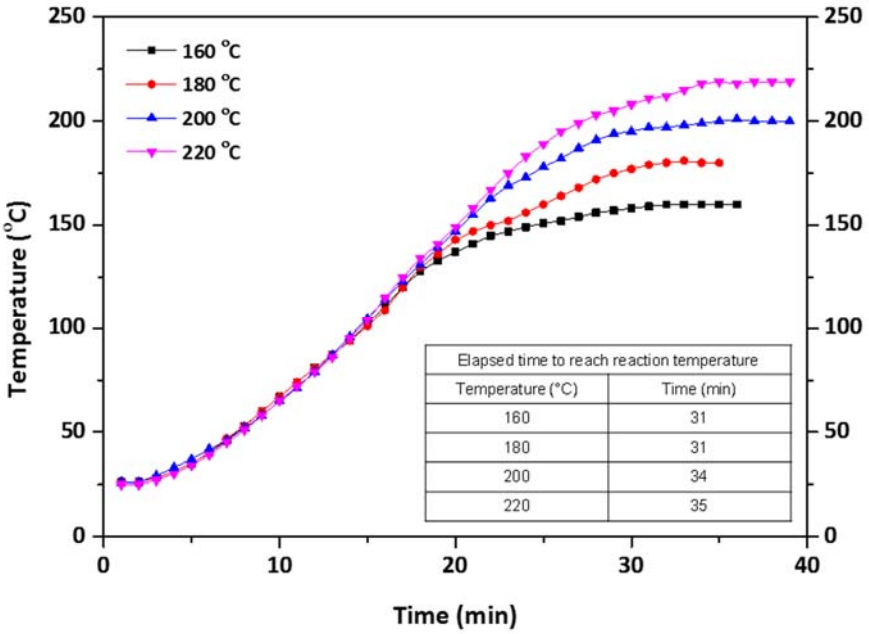

Elapsed time to reach reaction temperature	
Temperature (°C)	Time (min)
160	31
180	31
200	34
220	35

Figure 4-1. Temperature profile of a reactor for different target temperatures. Reactor volume= 50 mL, water= 30 mL, stirring speed= 600 rpm.

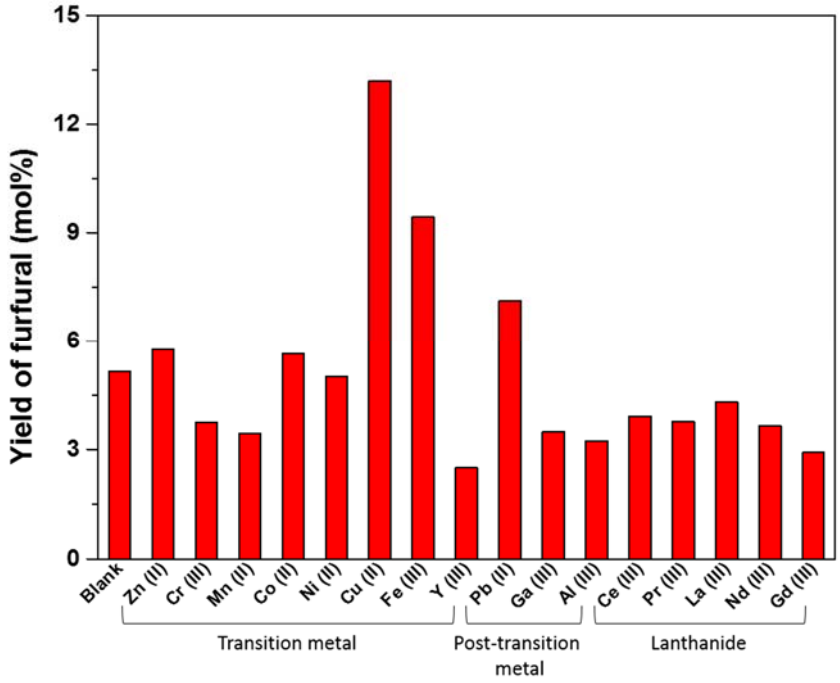

Figure 4-2. Catalytic performance of metal cations for the conversion of alginic acid to furfural at 200 °C for 30 min.

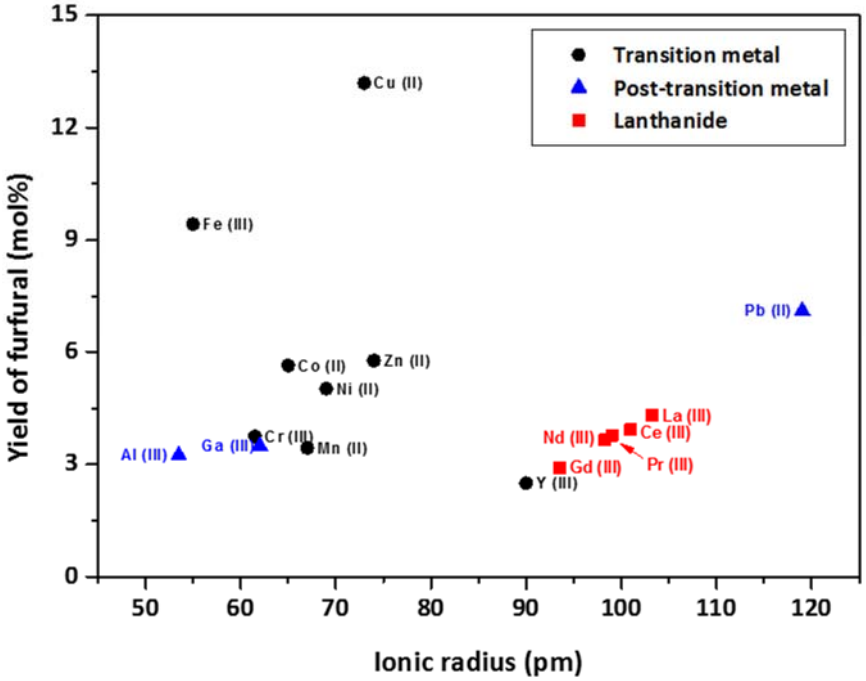

Figure 4-3. Influence of ionic radius of metal ions on the yield of furfural produced at 200 °C for 30 min.

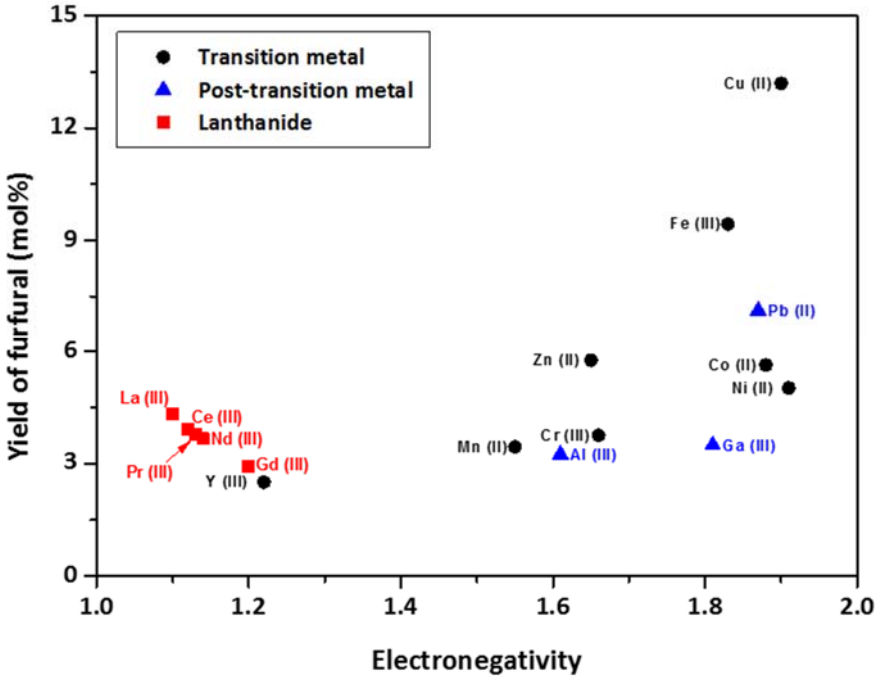

Figure 4-4. Effect of Pauling electronegativity of metal ions on the yield of furfural produced at 200 °C for 30 min.

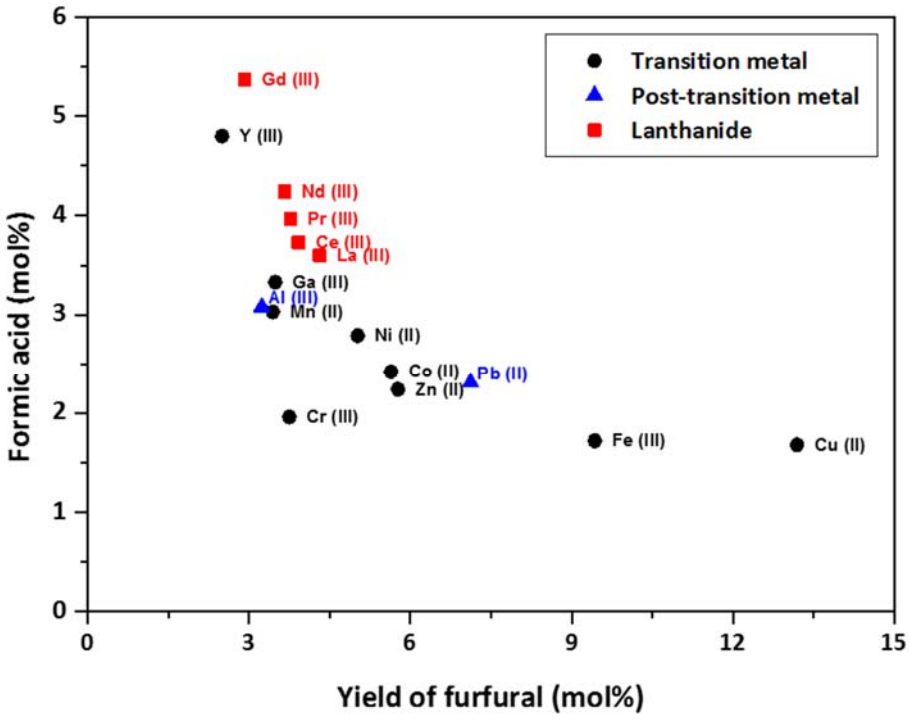

Figure 4-5. Correlation between yields of furfural and formic acid produced in the conversion of alginic acid under various metal cations at 200 °C for 30 min.

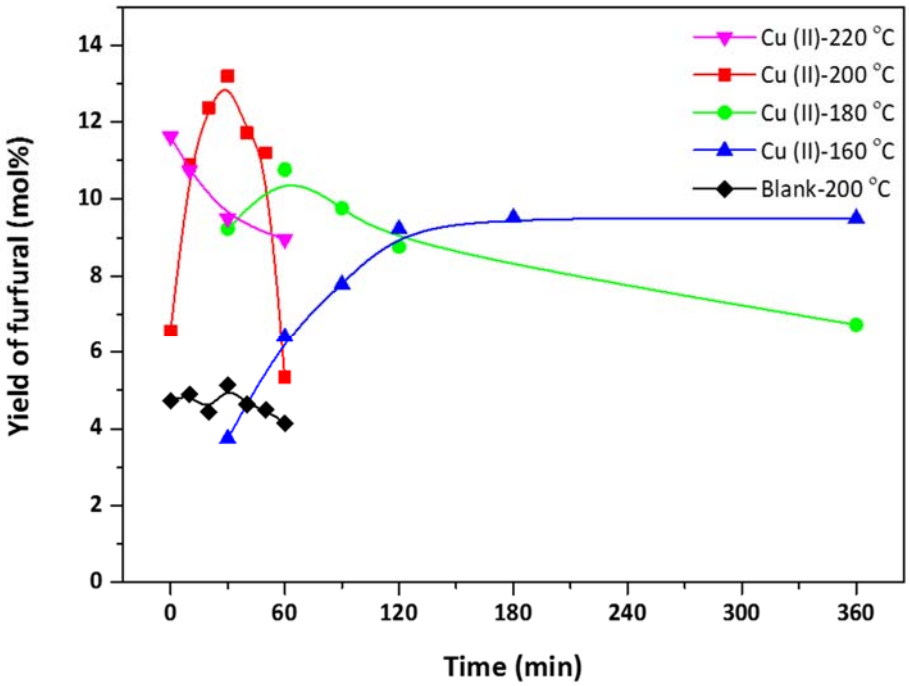

Figure 4-6. Effect of reaction temperature and time on the conversion of alginic acid to furfural catalyzed by Cu (II) ions.

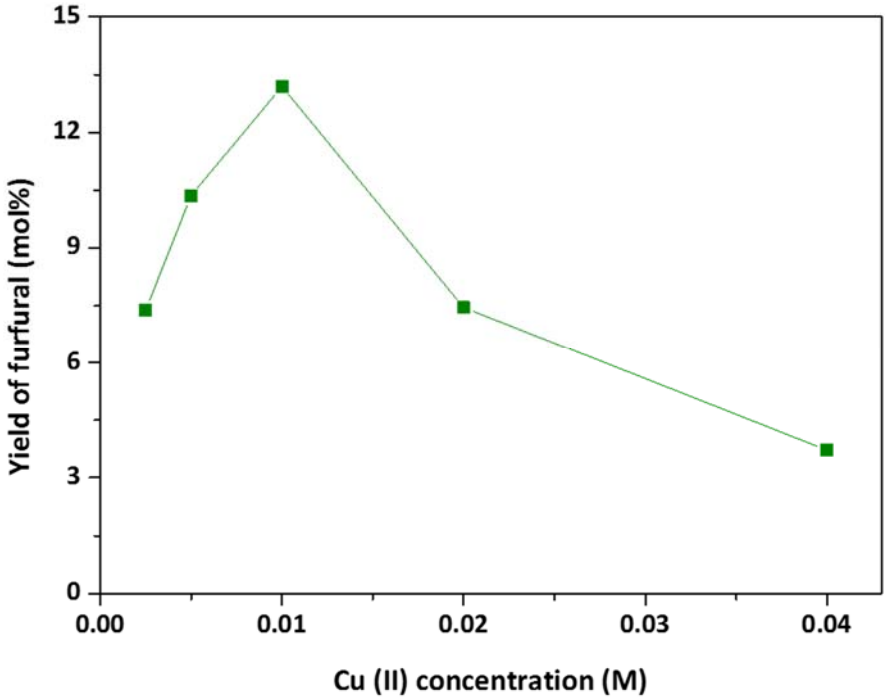

Figure 4-7. Yield of furfural produced by the hydrothermal reaction of alginic acid under Cu (II) ions with different concentrations.

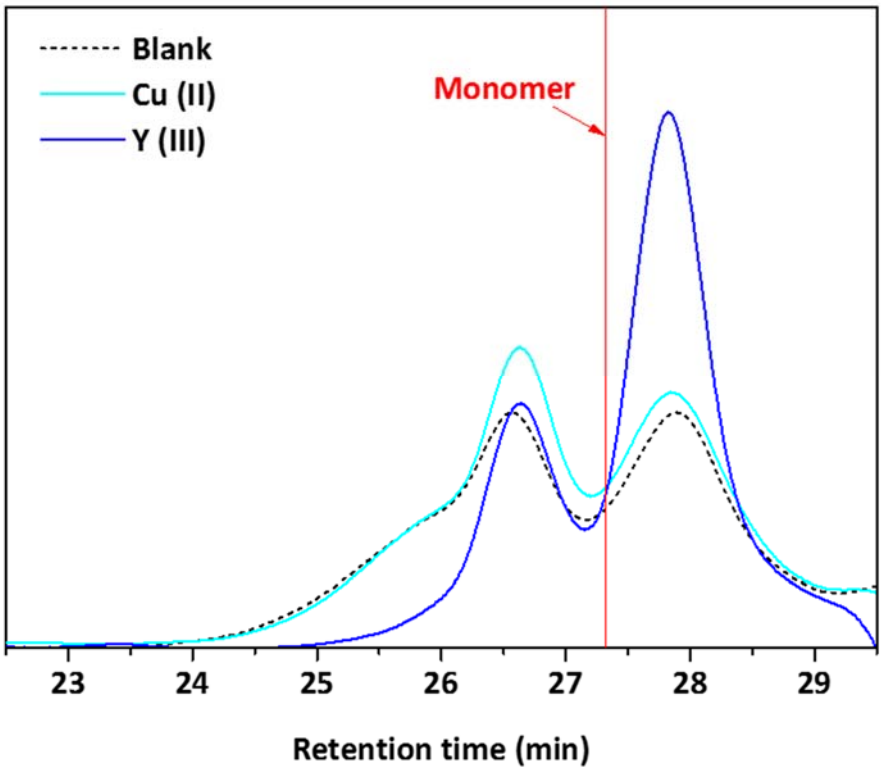

Figure 4-8. GPC chromatograms of liquid products obtained by the hydrothermal treatment of alginic acid under Cu (II) and Y (III) ions at 200 °C for 30 min.

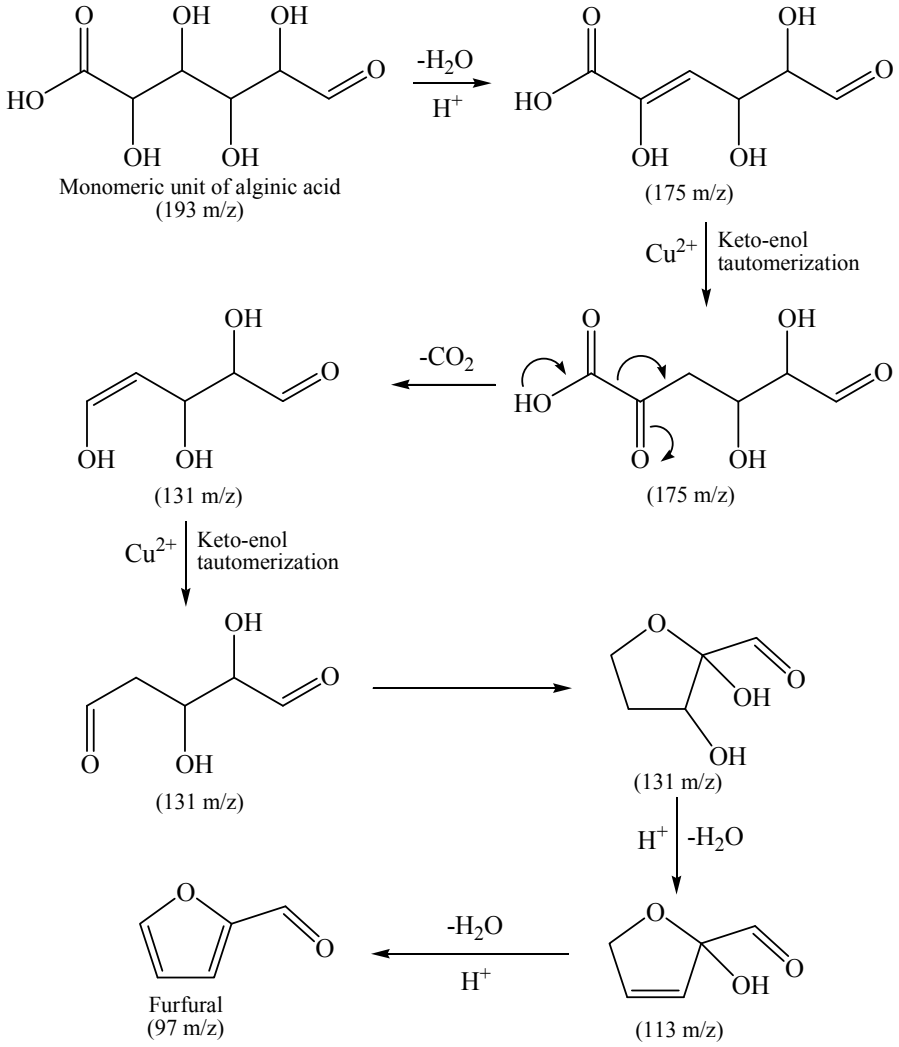

Figure 4-9. Proposed reaction pathway of the furfural production from monomer of alginic acid catalyzed by Cu (II) ions.

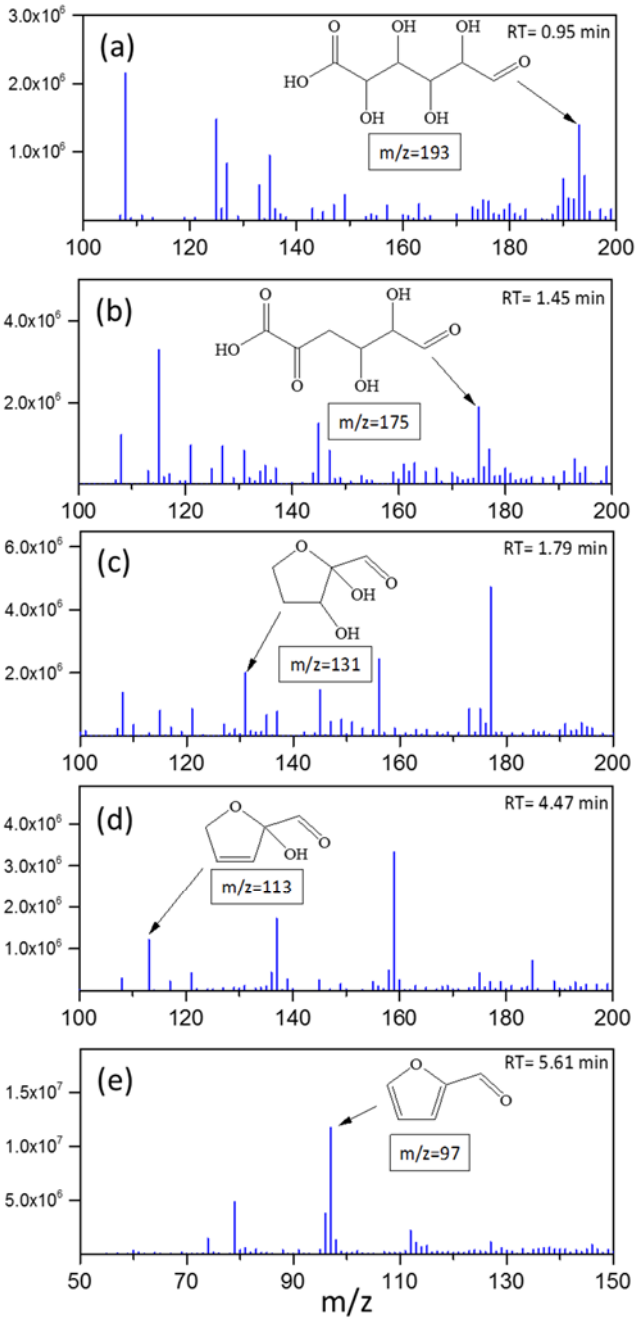

Figure 4-10. LC-MS spectra of product obtained by the hydrothermal treatment of alginic acid catalyzed by Cu (II) ions at 200 °C for 30 min. (a, b, c, d) negative ionization mode, (d) positive ionization mode.

Chapter 5. Summary and Conclusions

The hydrothermal treatment of alginate was performed with controlling pH of aqueous reaction medium in order to study the effects of acidity and basicity on the production of value-added chemicals. The pH level controlled by Arrhenius acid and base was used as a quantitative standard indicating acidity and basicity of the aqueous reaction medium. A base-catalyzed reaction at pH 13 promotes the decomposition of alginate, resulting in the production of lactic acid, fumaric acid and malic acid as major species. At pH 1, monomers (mannuronicacid and guluronic acid), furfural and glycolic acid are predominantly produced by the acid-catalyzed hydrothermal decomposition of alginate. Increasing the reaction temperature also enhances both the acid- and base-catalyzed reactions, however, the product distribution is strongly dependent on the acidity and basicity of reaction solvent. In other words, the acid and base catalysts significantly influence in determining the distribution of final products, whereas the reaction temperature is a more important factor for reducing the molecular weight of alginate in hydrothermal conditions. The selective production of value-added organic compounds can be achieved by carefully adjusting the reaction conditions such as pH, temperature and time.

For the selective production of lactic acid from alginate, the hydrothermal treatment of alginate was conducted with using metal oxides as a solid base catalyst. The metal oxides catalysts used in the hydrothermal reaction are Al_2O_3, MgO, Mg-Al mixed oxides, CaO, ZnO, ZrO_2, CeO_2 and TiO_2. Among these metal oxides, CaO exhibited the best catalytic performance, with a maximum lactic acid yield (12.66%) at 200 °C after 1 h. The lactic acid yield with the CaO catalyst is two times higher than with the traditional homogeneous base catalyst,

NaOH. The differences in the catalytic activities of the metal oxide catalysts are attributed to the basicity of the catalysts measured by titration and CO_2-TPD. The high density of medium basic sites on CaO seems to play a role of active sites promoting the dissociative adsorption of water, which provides the Brønsted base that catalyzes the hydrothermal conversion of alginate to lactic acid. During the reaction, it was observed that CaO was partially transformed to $Ca(OH)_2$ by the hydration reaction in the aqueous reaction medium. After the second run, the catalytic activity of CaO decreased to less than half the yield of lactic acid in the first run, due to the depletion of Brønsted base (OH^-) caused by which unreacted alginate and organic products covered the active site of CaO. However, the original catalytic activity was successfully recovered by recalcination of the deactivated CaO catalyst. Plausible reaction pathways for the production of lactic acid and α-hydroxyglutaric acid were proposed to describe the role of the CaO catalyst in the hydrothermal conversion of alginate. The CaO catalyst seems to promote the Benzilic acid rearrangement reaction with the dissociative adsorption of water molecules. The hydrothermal treatment of alginate using the CaO catalyst demonstrates high potential that macroalgae-derived alginate can be used to produce lactic acid as a renewable alternative feedstock.

The hydrothermal treatment of alginic acid was conducted under metal cations in order to study the effect of metal cations on the production of furfural. Among various metal ions, Cu (II) ions showed the highest furfural yield (13.19 %) at 200 °C for 30 min. The yield of furfural is proportional to the electronegativity of metal ions, however, the relationship between the furfural yield and the size of metal ions is not clear. The production of furfural from alginic acid is strongly dependent on the experimental conditions, such as

temperature, time and concentration of metal ions. From the results of GPC analysis, it is found that the high degree of depolymerization cannot guarantee the high furfural yield. The proposed reaction pathway demonstrates that the elimination of carbon dioxide by the decarboxylation reaction is an essential reaction step for the conversion of alginic acid to furfural. The decarboxylation reaction is initiated by the tautomerization reaction catalyzed by the interaction between the electrons of oxygen atoms and the electronegative metal ions. The catalytic hydrothermal conversion of alginic acid to furfural exhibits a promising potential that the macroalgae-derived alginic acid can be utilized as a renewable alternative feedstock, instead of hemicellulosic biomass, for the production of furfural.

Bibliography

1. Lashof, D.A. and D.R. Ahuja, *Nature*, **1990**, 344, 529-531.
2. Barbir, F., T.N. Veziroğlu, and H.J. Plass Jr, *International Journal of Hydrogen Energy*, **1990**, 15, 739-749.
3. Likens, G.E., F.H. Bormann, and N.M. Johnson, *Environment: Science and Policy for Sustainable Development*, **1972**, 14, 33-40.
4. Hoel, M. and S. Kverndokk, *Resource and Energy Economics*, **1996**, 18, 115-136.
5. Withagen, C., *Resource and Energy Economics*, **1994**, 16, 235-242.
6. John, R.P., G.S. Anisha, K.M. Nampoothiri, and A. Pandey, *Bioresource Technology*, **2011**, 102, 186-193.
7. Wei, N., J. Quarterman, and Y.-S. Jin, *Trends in Biotechnology*, **2013**, 31, 70-77.
8. Baghel, R.S., N. Trivedi, V. Gupta, A. Neori, C.R.K. Reddy, A. Lali, and B. Jha, *Green Chemistry*, **2015**, 17, 2436-2443.
9. Faber, M.D., *Enzyme and Microbial Technology*, **1979**, 1, 226-232.
10. Xu, C., R.A.D. Arancon, J. Labidi, and R. Luque, *Chemical Society Reviews*, **2014**, 43, 7485-7500.
11. Williams, P.J.l.B. and L.M.L. Laurens, *Energy & Environmental Science*, **2010**, 3, 554-590.
12. Enquist-Newman, M., A.M.E. Faust, D.D. Bravo, C.N.S. Santos, R.M. Raisner, A. Hanel, P. Sarvabhowman, C. Le, D.D. Regitsky, S.R. Cooper, L. Peereboom, A. Clark, Y. Martinez, J. Goldsmith, M.Y. Cho, P.D. Donohoue, L. Luo, B. Lamberson, P. Tamrakar, E.J. Kim, J.L. Villari, A. Gill, S.A. Tripathi, P. Karamchedu, C.J. Paredes, V.

Rajgarhia, H.K. Kotlar, R.B. Bailey, D.J. Miller, N.L. Ohler, C. Swimmer, and Y. Yoshikuni, *Nature*, **2014**, 505, 239-243.

13. Shen, Z., J. Zhou, X. Zhou, and Y. Zhang, *Applied Energy*, **2011**, 88, 3444-3447.
14. Chisti, Y., *Biotechnology Advances*, **2007**, 25, 294-306.
15. Chisti, Y., *Trends in Biotechnology*, **2008**, 26, 126-131.
16. Mata, T.M., A.A. Martins, and N.S. Caetano, *Renewable and Sustainable Energy Reviews*, **2010**, 14, 217-232.
17. Klass, D.L., *Biomass for Renewable Energy, Fuels, and Chemicals*. 1998: Acedemic Press.
18. Larsen, B., D.M.S.A. Salem, M.A.E. Sallam, M.M. Mishrikey, and A.I. Beltagy, *Carbohydrate Research*, **2003**, 338, 2325-2336.
19. Draget, K.I., O. Smidsrød, and G. Skjåk-Bræk, *Alginates from Algae*, in *Biopolymers Online*. 2005, Wiley-VCH Verlag GmbH & Co. KGaA.
20. Fischer, F.G. and H. Dörfel, *Die Polyuronsäuren Der Braunalgen (Kohlenhydrate Der Algen I)*, in *Hoppe-Seyler´s Zeitschrift für physiologische Chemie*. 1955. p. 186.
21. Arne Haug, B.L., *Acta Chem. Scand.*, **1962**, 16, 1908-1918.
22. Arne Haug, B.L.a.O.S., *Acta Chemica Scandinavica*, **1963**, 17, 1466-1468.
23. Sasaki, M., B. Kabyemela, R. Malaluan, S. Hirose, N. Takeda, T. Adschiri, and K. Arai, *The Journal of Supercritical Fluids*, **1998**, 13, 261-268.
24. Zhao, H., J.H. Kwak, Y. Wang, J.A. Franz, J.M. White, and J.E. Holladay, *Energy & Fuels*, **2005**, 20, 807-811.
25. Peterson, A.A., F. Vogel, R.P. Lachance, M. Froling, J.M.J. Antal, and

J.W. Tester, *Energy & Environmental Science*, **2008**, 1, 32-65.

26. Möller , M., P. Nilges , F. Harnisch, and U. Schröder, *Chemsuschem*, **2011**, 4, 566-579.
27. Toor, S.S., L. Rosendahl, and A. Rudolf, *Energy*, **2011**, 36, 2328-2342.
28. Kabyemela, B.M., T. Adschiri, R.M. Malaluan, and K. Arai, *Industrial & Engineering Chemistry Research*, **1997**, 36, 1552-1558.
29. Kabyemela, B.M., T. Adschiri, R. Malaluan, and K. Arai, *Industrial & Engineering Chemistry Research*, **1997**, 36, 2025-2030.
30. Kabyemela, B.M., T. Adschiri, R.M. Malaluan, and K. Arai, *Industrial & Engineering Chemistry Research*, **1999**, 38, 2888-2895.
31. Srokol, Z., A.-G. Bouche, A. van Estrik, R.C.J. Strik, T. Maschmeyer, and J.A. Peters, *Carbohydrate Research*, **2004**, 339, 1717-1726.
32. Salak Asghari, F. and H. Yoshida, *Industrial & Engineering Chemistry Research*, **2006**, 45, 2163-2173.
33. Russell, J.A., R.K. Miller, and P.M. Molton, *Biomass*, **1983**, 3, 43-57.
34. Luijkx, G.C.A., F. van Rantwijk, and H. van Bekkum, *Carbohydrate Research*, **1993**, 242, 131-139.
35. Kruse, A., *Biofuels, Bioproducts and Biorefining*, **2008**, 2, 415-437.
36. Williams, P.T. and J. Onwudili, *Energy & Fuels*, **2006**, 20, 1259-1265.
37. Matsumura, Y., T. Minowa, B. Potic, S.R.A. Kersten, W. Prins, W.P.M. van Swaaij, B. van de Beld, D.C. Elliott, G.G. Neuenschwander, A. Kruse, and M. Jerry Antal Jr, *Biomass and Bioenergy*, **2005**, 29, 269-292.
38. Yin, S., Y. Pan, and Z. Tan, *International Journal of Green Energy*, **2011**, 8, 234-247.
39. Adschiri, T., *Chemistry Letters*, **2007**, 36, 1188-1193.

40. Jin, F.M., J. Yun, G.M. Li, A. Kishita, K. Tohji, and H. Enomoto, *Green Chemistry*, **2008**, 10, 612-615.

41. Anastasakis, K. and A.B. Ross, *Bioresource Technology*, **2011**, 102, 4876-4883.

42. Bicker, M., S. Endres, L. Ott, and H. Vogel, *Journal of Molecular Catalysis A: Chemical*, **2005**, 239, 151-157.

43. Huang, Y.-B. and Y. Fu, *Green Chemistry*, **2013**, 15, 1095-1111.

44. Rinaldi, R. and F. Schüth, *Chemsuschem*, **2009**, 2, 1096-1107.

45. Dhepe, P.L. and A. Fukuoka, *Chemsuschem*, **2008**, 1, 969-975.

46. Klemm, D., B. Heublein, H.-P. Fink, and A. Bohn, *Angewandte Chemie*, **2005**, 117, 3422-3458.

47. Gacesa, P., A. Squire, and P.J. Winterburn, *Carbohydrate Research*, **1983**, 118, 1-8.

48. Grasdalen, H., B. Larsen, and O. Smidsrød, *Carbohydrate Research*, **1979**, 68, 23-31.

49. Niemela, K. and E. Sjostrom, *Carbohydrate Research*, **1985**, 144, 241-249.

50. Aida, T.M., T. Yamagata, M. Watanabe, and R.L. Smith, *Carbohydrate Polymers*, **2010**, 80, 296-302.

51. Aida, T.M., T. Yamagata, C. Abe, H. Kawanami, M. Watanabe, and R.L. Smith, *Journal of Supercritical Fluids*, **2012**, 65, 39-44.

52. Esposito, D. and M. Antonietti, *Chemsuschem*, **2013**, 6, 989-992.

53. Dee, S.J. and A.T. Bell, *Chemsuschem*, **2011**, 4, 1166-1173.

54. Qi, X., H. Guo, L. Li, and R.L. Smith, *Chemsuschem*, **2012**, 5, 2215-2220.

55. Tao, F., H. Song, and L. Chou, *Journal of Molecular Catalysis A:*

Chemical, **2012**, 357, 11-18.

56. Jiang, F., Q. Zhu, D. Ma, X. Liu, and X. Han, *Journal of Molecular Catalysis A: Chemical*, **2011**, 334, 8-12.
57. Yadav, K.K., S. Ahmad, and S.M.S. Chauhan, *Journal of Molecular Catalysis A: Chemical*, **2014**, 394, 170-176.
58. Arne Haug, B.L., Olav Smidsrød, *Acta Chemica Scandinavica*, **1966**, 20, 8.
59. Arne Haug, B.L., Olav Smidsrød, *Acta Chemica Scandinavica*, **1967**, 21, 12.
60. Akiya, N. and P.E. Savage, *Chemical Reviews*, **2002**, 102, 2725-2750.
61. Niemelä, K. and E. Sjöström, *Carbohydrate Research*, **1985**, 144, 93-99.
62. Granados, M.L., A.C. Alba-Rubio, I. Sadaba, R. Mariscal, I. Mateos-Aparicio, and A. Heras, *Green Chemistry*, **2011**, 13, 3203-3212.
63. Danon, B., G. Marcotullio, and W. de Jong, *Green Chemistry*, **2014**, 16, 39-54.
64. Lira, C.T. and P.J. McCrackin, *Industrial & Engineering Chemistry Research*, **1993**, 32, 2608-2613.
65. Sánchez, C., I. Egüés, A. García, R. Llano-Ponte, and J. Labidi, *Chemical Engineering Journal*, **2012**, 181–182, 655-660.
66. Alonso, D.M., J.Q. Bond, and J.A. Dumesic, *Green Chemistry*, **2010**, 12, 1493-1513.
67. Gallezot, P., *Chemical Society Reviews*, **2012**, 41, 1538-1558.
68. Bozell, J.J. and G.R. Petersen, *Green Chemistry*, **2010**, 12, 539-554.
69. Werpy, T. and G. Petersen, *U. S. Department of Energy*, **2004**, 1, 1-76.
70. Dusselier, M., P. Van Wouwe, A. Dewaele, E. Makshina, and B.F. Sels,

Energy & Environmental Science, **2013**, 6, 1415-1442.

71. Corma, A., S. Iborra, and A. Velty, *Chemical Reviews*, **2007**, 107, 2411-2502.

72. Fan, Y., C. Zhou, and X. Zhu, *Catalysis Reviews*, **2009**, 51, 293-324.

73. Carlos Serrano-Ruiz, J. and J.A. Dumesic, *Green Chemistry*, **2009**, 11, 1101-1104.

74. Jin, F. and H. Enomoto, *Energy & Environmental Science*, **2011**, 4, 382-397.

75. Datta, R. and M. Henry, *Journal of Chemical Technology & Biotechnology*, **2006**, 81, 1119-1129.

76. Yan, X., F. Jin, K. Tohji, A. Kishita, and H. Enomoto, *AIChE Journal*, **2010**, 56, 2727-2733.

77. Wang, Y., W. Deng, B. Wang, Q. Zhang, X. Wan, Z. Tang, Y. Wang, C. Zhu, Z. Cao, G. Wang, and H. Wan, *Nature Commnunications*, **2013**, 4, 1-7.

78. Whistler, R.L. and J.N. BeMiller, *Journal of the American Chemical Society*, **1960**, 82, 457-459.

79. Jeon, W., C. Ban, G. Park, T.-K. Yu, J.-Y. Suh, H.C. Woo, and D.H. Kim, *Journal of Molecular Catalysis A: Chemical*, **2015**, 399, 106-113.

80. Liu, Z., W. Li, C. Pan, P. Chen, H. Lou, and X. Zheng, *Catalysis Communications*, **2011**, 15, 82-87.

81. Di Cosimo, J.I., V.K. Díez, M. Xu, E. Iglesia, and C.R. Apesteguía, *Journal of Catalysis*, **1998**, 178, 499-510.

82. Xie, W., H. Peng, and L. Chen, *Journal of Molecular Catalysis A: Chemical*, **2006**, 246, 24-32.

83. Liu, X., H. He, Y. Wang, S. Zhu, and X. Piao, *Fuel*, **2008**, 87, 216-221.

84. Onda, A., T. Ochi, K. Kajiyoshi, and K. Yanagisawa, *Catalysis Communications*, **2008**, 9, 1050-1053.

85. Choudhary, H., S. Nishimura, and K. Ebitani, *Applied Catalysis B: Environmental*, **2015**, 162, 1-10.

86. Venkat Reddy, C.R., R. Oshel, and J.G. Verkade, *Energy & Fuels*, **2006**, 20, 1310-1314.

87. Deng, X., Z. Fang, Y.-h. Liu, and C.-L. Yu, *Energy*, **2011**, 36, 777-784.

88. Jin, F., Z. Zhou, H. Enomoto, T. Moriya, and H. Higashijima, *Chemistry Letters*, **2004**, 33, 126-127.

89. Haug, A., B. Larsen, and O. Smidsrod, *Carbohydrate Research*, **1974**, 32, 217-225.

90. Pham, H.D., J. Seon, S.C. Lee, M. Song, and H.-C. Woo, *Bioresource Technology*, **2013**, 148, 601-604.

91. Seon, J., T. Lee, S.C. Lee, H.D. Pham, H.C. Woo, and M. Song, *Bioresource Technology*, **2014**, 157, 22-27.

92. Takeda, H., F. Yoneyama, S. Kawai, W. Hashimoto, and K. Murata, *Energy & Environmental Science*, **2011**, 4, 2575-2581.

93. Wargacki, A.J., E. Leonard, M.N. Win, D.D. Regitsky, C.N.S. Santos, P.B. Kim, S.R. Cooper, R.M. Raisner, A. Herman, A.B. Sivitz, A. Lakshmanaswamy, Y. Kashiyama, D. Baker, and Y. Yoshikuni, *Science*, **2012**, 335, 308-313.

94. Chheda, J.N., G.W. Huber, and J.A. Dumesic, *Angewandte Chemie-International Edition*, **2007**, 46, 7164-7183.

95. Yan, K., G. Wu, T. Lafleur, and C. Jarvis, *Renewable and Sustainable Energy Reviews*, **2014**, 38, 663-676.

96. Mamman, A.S., J.-M. Lee, Y.-C. Kim, I.T. Hwang, N.-J. Park, Y.K.

Hwang, J.-S. Chang, and J.-S. Hwang, *Biofuels, Bioproducts and Biorefining*, **2008**, 2, 438-454.

97. Karinen, R., K. Vilonen, and M. Niemelä, *Chemsuschem*, **2011**, 4, 1002-1016.

98. Dutta, S., S. De, B. Saha, and M.I. Alam, *Catalysis Science & Technology*, **2012**, 2, 2025-2036.

99. Climent, M.J., A. Corma, and S. Iborra, *Green Chemistry*, **2011**, 13, 520-540.

100. Choudhary, V., S.I. Sandler, and D.G. Vlachos, *ACS Catalysis*, **2012**, 2, 2022-2028.

101. Sahu, R. and P.L. Dhepe, *Chemsuschem*, **2012**, 5, 751-761.

102. García-Sancho, C., J.M. Rubio-Caballero, J.M. Mérida-Robles, R. Moreno-Tost, J. Santamaría-González, and P. Maireles-Torres, *Catalysis Today*, **2014**, 234, 119-124.

103. Bhaumik, P. and P.L. Dhepe, *Catalysis Today*, **2015**, 251, 66-72.

104. Marcotullio, G. and W. de Jong, *Carbohydrate Research*, **2011**, 346, 1291-1293.

105. Agirrezabal-Telleria, I., J. Requies, M.B. Güemez, and P.L. Arias, *Applied Catalysis B: Environmental*, **2014**, 145, 34-42.

106. Takagaki, A., M. Ohara, S. Nishimura, and K. Ebitani, *Chemical Communications*, **2009**, 6276-6278.

107. Tao, F., H. Song, and L. Chou, *Carbohydrate Research*, **2011**, 346, 58-63.

108. Boffa, A., C. Lin, A.T. Bell, and G.A. Somorjai, *Journal of Catalysis*, **1994**, 149, 149-158.

109. Papageorgiou, S.K., E.P. Kouvelos, E.P. Favvas, A.A. Sapalidis, G.E.

Romanos, and F.K. Katsaros, *Carbohydrate Research*, **2010**, 345, 469-473.

110. Yemiş, O. and G. Mazza, *Bioresource Technology*, **2011**, 102, 7371-7378.

111. Yang, W., P. Li, D. Bo, and H. Chang, *Carbohydrate Research*, **2012**, 357, 53-61.

112. Huo, Z., Y. Fang, D. Ren, S. Zhang, G. Yao, X. Zeng, and F. Jin, *ACS Sustainable Chemistry & Engineering*, **2014**, 2, 2765-2771.

국 문 초 록

최근 들어 바이오연료 및 유용한 화합물 생산을 위한 재생가능 원료로서 해조류 바이오매스가 주목을 받고 있다. 해조류 바이오매스는 기존의 바이오매스 (옥수수, 사탕수수 및 목질계 바이오매스)와 비교하여, 생장속도가 빠르고 난분해성 리그닌 성분이 없기 때문에 재생가능한 바이오매스자원으로서 큰 이점이 있다. 이러한 해조류 바이오매스는 미세조류와 거대조류로 분류할 수 있는데, 지질성분의 함량이 높은 미세조류는 바이오디젤 생산분야에서 활발히 연구되고 있다. 이에 반해, 알지네이트 (alginate) 또는 마니톨 (mannitol)과 같은 탄수화물로 구성된 거대조류는 바이오오일, 휘발성 지방산 및 바이오알코올과 같은 물질을 생산하는 연구에 주로 활용되고 있다. 거대조류를 구성하는 주요 성분 중의 하나인 알지네이트는 β-D-만루론산 (β-D-mannuronic acid)과 α-L-글루론산 (α-L-guluronic acid)의 글리코시딕 결합 (glycosidic linkage)에 의해서 이루어진 고분자 물질로 셀룰로오스 (cellulose)와 유사한 구조적 특징을 갖는다. 따라서 셀룰로오스를 고부가가치화하는 열화학적 또는 생물학적 전환공정에 알지네이트를 적용할 수 있는 방법이 연구되고 있다. 다양한 전환공정 가운데, 수열전환공정 (hydrothermal conversion process)은 물을 반응매개체로 사용하기 때문에, 비교적 경제적이고 친환경적인 바이오매스 전환기술로서 주목받고 있다.

본 연구에서는 수열전환기법을 이용하여, 알지네이트로부터 고부가가치의 화합물을 생산하기 위한 촉매반응을 수행하였다. 반응매개체인 물의 산도 (acidity) 및 염기도 (basicity)가

알지네이트의 수열반응에 미치는 영향을 알아보기 위해, 아레니우스 산 및 염기(Arrhenius acid and base)를 사용하여 반응물의 초기 pH 를 1 부터 13 까지 조절한 다음, 150 °C 부터 250 °C 의 반응온도에서 실험을 수행하였다. 그 결과, 염기도가 높을수록 (pH 13) 알지네이트의 분해가 활발히 일어나며, 최종생성물 중에서 젖산(lactic acid), 푸마르산 (fumaric acid) 및 말산 (malic acid)의 함량이 높은 것을 확인하였다. 이에 반해, 높은 산도 (pH 1)에서는 알지네이트의 단량체, 푸르푸랄 (furfural) 및 글리콜산 (glycolic acid)의 수율이 높게 나타나는 것이 관찰되었다. 반응온도가 높아짐에 따라, 산 또는 염기촉매가 첨가되지 않은 중성의 반응조건에서도 산 또는 염기촉매반응이 일어남을 알 수 있었는데, 이는 고온-고압상태에서 발생하는 물의 해리작용에 의해 이온 곱 (ion product, K_w)의 수치가 상승하기 때문이라고 할 수 있다. 위 실험을 통해서, 반응용매의 산도, 염기도 및 반응온도가 알지네이트 수열반응 결과에 지대한 영향을 미친다는 것을 확인하였다.

그리고 알지네이트로부터 젖산을 선택적으로 생산하기 위한 촉매반응에 관한 실험을 수행하였다. 젖산의 선택적 생산을 위한 촉매로는 다양한 금속 산화물이 사용되었는데, CaO 촉매를 이용하여 200 °C 에서 6 시간 동안 반응했을 때 가장 높은 젖산의 수율 (14.66 %)을 얻을 수 있었다. 이에 반해, 다른 금속 산화물 촉매를 사용한 경우에는 젖산의 수율이 대체로 낮게 측정이 되었다. 촉매의 적정(titration)을 통해 염기도를 측정한 결과, 젖산의 수율은 촉매로부터 발생하는 브뢴스테드 염기 (Brønsted base)의 개체수에 비례함을 알 수 있었다. 재사용성을 평가한 결과, CaO 촉매는 촉매활성의 저하 없이 연속적으로 두 차례 사용이 가능하였으며, 저하된 촉매활성은 열처리를 통해서 초기의 활성으로 회복되었다.

이러한 촉매의 활성저하는 부반응물이 촉매의 활성점인 루이스 산점 (Lewis acid site) 및 브뢴스테드 염기점 (Brønsted base site)을 덮음으로써, 반응물과 활성점과의 접촉을 저해하기 때문에 발생하는 것으로 판단된다. 이러한 실험결과 및 분석결과를 바탕으로, CaO 촉매 하에서 알지네이트로부터 젖산이 생성되는 반응경로를 제안하였다. 추가적으로, 촉매가 알지네이트의 분자량 분포변화에 미치는 영향을 분석하였다.

알긴산으로부터 푸르푸랄을 선택적으로 생산하기 위해서 다양한 금속 양이온을 촉매로 사용하였는데, 200 °C 의 반응온도에서 30 분간 반응을 수행한 결과, 구리 (II) 이온을 촉매로 사용한 경우에 가장 높은 푸르푸랄 수율 (13.19%)을 얻을 수 있다. 구리이온을 첨가한 상태에서, 반응온도와 시간이 푸르푸랄 수율에 미치는 영향을 관찰하였는데, 수율이 반응온도에 비례하여 증가하다가 일정시간 이후에 감소하는 것을 확인하였다. 수율 감소의 원인은, 반응이 지속됨에 따라 생성된 푸르푸랄이 휴민 (humin) 또는 기타 유기산으로 전환되기 때문이다. 또한, 푸르푸랄 수율은 구리이온의 농도에 따라 민감하게 변화하였는데, 구리이온의 농도가 0.01 M 일 때 가장 높은 푸르푸랄 수율을 보였다. 금속이온 촉매와 반응조건이 수열반응에 의한 알긴산의 분자량 변화에 미치는 영향을 젤 투과 크로마토그래피 기법을 이용하여 분석하였으며, 액체크로마토그래피와 질량분석기를 이용한 생성물 분석을 통해서 푸르푸랄의 생성반응경로를 제안하였다.

주요어: 알지네이트, 수열반응, 균일계 촉매, 불균일계 촉매, 유기산, 푸르푸랄

학번: 2012-30259